

1 **Recent increases in the atmospheric growth rate and emissions of HFC-23** 2 **(CHF₃) and the link to HCFC-22 (CHClF₂) production**

3 Peter G. Simmonds¹, Matthew Rigby¹, Archie McCulloch¹, Martin K. Vollmer², Stephan
4 Henne², Jens Mühle³, Simon O'Doherty¹, Alistair J. Manning⁴, Paul B. Krummel⁵, Paul J.
5 Fraser⁵, Dickon Young¹, Ray F. Weiss³, Peter K. Salameh³, Christina M. Harth³, Stefan
6 Reimann², Cathy M. Trudinger⁵, L. Paul Steele⁵, Ray H. J. Wang⁶, Diane J. Ivy⁷, Ronald G.
7 Prinn⁷, Blagoj Mitrevski⁵, and David M. Etheridge⁵.

8
9 ¹ Atmospheric Chemistry Research Group, University of Bristol, Bristol, UK

10 ² Swiss Federal Laboratories for Materials Science and Technology, Laboratory for Air Pollution
11 and Environmental Technology (Empa), Dübendorf, Switzerland,

12 ³ Scripps Institution of Oceanography (SIO), University of California at San Diego, La Jolla,
13 California, USA

14 ⁴ Met Office Hadley Centre, Exeter, UK

15 ⁵ Climate Science Centre, Commonwealth Scientific and Industrial Research Organisation
16 (CSIRO) Oceans and Atmosphere, Aspendale, Victoria, Australia

17 ⁶ School of Earth, and Atmospheric Sciences, Georgia Institute of Technology, Atlanta, Georgia,
18 USA

19 ⁷ Center for Global Change Science, Massachusetts Institute of Technology, Cambridge,
20 Massachusetts, USA

21
22 Correspondence to: P.G. Simmonds (petersimmonds@aol.com)

23 **Abstract**

25 High frequency measurements of trifluoromethane (HFC-23, CHF₃), a potent hydrofluorocarbon
26 greenhouse gas, largely emitted to the atmosphere as by-product of production of the
27 hydrochlorofluorocarbon HCFC-22 (CHClF₂), at five core stations of the Advanced Global
28 Atmospheric Gases Experiment (AGAGE) network, combined with measurements on firn air,
29 old Northern Hemisphere air samples and Cape Grim Air Archive (CGAA) air samples, are used
30 to explore the current and historic changes in the atmospheric abundance of HFC-23. These
31 measurements are used in combination with the AGAGE 2-D atmospheric 12-box model and a
32 Bayesian inversion methodology to determine model atmospheric mole fractions and the history
33 of global HFC-23 emissions. The global modelled annual mole fraction of HFC-23 in the
34 background atmosphere was 28.9 ± 0.6 pmol mol⁻¹ at the end of 2016, representing a 28%
35 increase from 22.6 ± 0.4 pmol mol⁻¹ in 2009. Over the same time frame, the modelled mole
36 fraction of HCFC-22 increased by 19% from 199 ± 2 pmol mol⁻¹ to 237 ± 2 pmol mol⁻¹.
37 However, unlike HFC-23, the annual average HCFC-22 growth rate slowed from 2009 to 2016
38 at an annual average rate of -0.5 pmol mol⁻¹ yr⁻². This slowing atmospheric growth is consistent
39 with HCFC-22 moving from dispersive (high fractional emissions) to feedstock (low fractional
40 emissions) uses, with HFC-23 emissions remaining as a consequence of incomplete mitigation
41 from all HCFC-22 production.

42

43 Our results demonstrate that, following a minimum in HFC-23 global emissions in 2009 of $9.6 \pm$
44 0.6 Gg yr^{-1} , emissions increased to a maximum in 2014 of $14.5 \pm 0.6 \text{ Gg yr}^{-1}$ and then declined
45 to $12.7 \pm 0.6 \text{ Gg yr}^{-1}$ ($157 \text{ Mt CO}_2\text{-e yr}^{-1}$) in 2016. The 2009 emissions minimum is consistent
46 with estimates based on national reports and is likely a response to the implementation of the
47 Clean Development Mechanism (CDM) to mitigate HFC-23 emissions by incineration in
48 developing (Non-Annex 1) countries under the Kyoto Protocol. Our derived cumulative
49 emissions of HFC-23 during 2010-2016 were $89 \pm 2 \text{ Gg}$ ($1.1 \pm 0.2 \text{ Gt CO}_2\text{-e}$), which led to an
50 increase in radiative forcing of $1.0 \pm 0.1 \text{ mW m}^{-2}$ over the same period. Although the CDM had
51 reduced global HFC-23 emissions, it cannot now offset the higher emissions from increasing
52 HCFC-22 production in Non-Annex 1 countries, as the CDM was closed to new entrants in
53 2009. We also find that the cumulative European HFC-23 emissions from 2010 to 2016 were
54 $\sim 1.3 \text{ Gg}$, corresponding to just 1.5% of cumulative global HFC-23 emissions over this same
55 period. The majority of the increase in global HFC-23 emissions since 2010 is attributed to a
56 delay in the adoption of mitigation technologies, predominantly in China and east Asia.
57 However, a reduction in emissions is anticipated, when the Kigali 2016 amendment to the
58 Montreal Protocol, requiring HCFC and HFC production facilities to introduce destruction of
59 HFC-23, is fully implemented.

60

61 **1. Introduction**

62 Due to concerns about climate change, trifluoromethane (CHF_3 , HFC-23) has attracted
63 interest as a potent greenhouse gas due to a 100-yr integrated global warming potential (GWP) of
64 12400 (Myhre et al., 2013) and an atmospheric lifetime of $\sim 228 \text{ yr}$ (SPARC, 2013).
65 Hydrofluorocarbons (HFCs) were introduced as replacements for ozone-depleting
66 chlorofluorocarbons (CFCs) and hydrochlorofluorocarbons (HCFCs) - for example, HFC-134a
67 as a direct replacement for CFC-12 (Xiang et al., 2014). However, HFC-23 is a by-product of
68 chlorodifluoromethane HCFC-22 (CHClF_2) production, resulting from the over-fluorination of
69 chloroform (CHCl_3). Most HFC-23 has historically been vented to the atmosphere (UNEP,
70 2017a). HFC-23 has also been used as a feed-stock in the production of Halon-1301 (CBrF_3)
71 (Miller and Batchelor, 2012) which substantially decreased with the phase-out of halons in 2010
72 under the Montreal Protocol, a landmark international agreement designed to protect the
73 stratospheric ozone layer. HFC-23 also has minor emissive uses in air conditioning, fire
74 extinguishers, and semi-conductor manufacture (McCulloch and Lindley, 2007) and very minor
75 emissions from aluminium production (Fraser et al., 2013). For developed countries HFC-23
76 emissions were controlled as part of the “F-basket” under the Kyoto Protocol, an international

77 treaty among industrialized nations that sets mandatory limits on greenhouse gas emissions,
78 (https://ec.europa.eu/clima/policies/f-gas_en).

79 In the context of this paper, we discuss “developed” and “developing” countries which
80 we take to be synonymous with Annex 1 (Non-Article 5) countries and Non-Annex 1 (Article 5)
81 countries, respectively.

82 There have been a number of previous publications related to HFC-23. Oram et al.
83 (1998) measured HFC-23 by gas chromatography-mass spectrometry (GC-MS) analysis of Cape
84 Grim flask air samples and sub-samples of the Cape Grim Air Archive (CGAA) from 1978-1995 and
85 reported a dry-air southern hemispheric atmospheric abundance of 11 pmol mol^{-1} in late-1995.
86 Culbertson et al. (2004) estimated global emissions of HFC-23 using a one-box model and GC-MS
87 analysis of north American and Antarctic air samples. A top-down HFC-23 emissions history and a
88 comprehensive bottom-up estimate of global HFC-23 emissions were reported by Miller et al.
89 (2010) using Advanced Global Atmospheric Gases Experiment (AGAGE) observations (2007-
90 2009) and samples from the CGAA (1978-2009). Montzka et al. (2010), using measurements of
91 firn air from the permeable upper layer of an ice sheet and ambient air collected during three
92 expeditions to Antarctica between 2001 and 2009, constructed a consistent Southern Hemisphere
93 (SH) atmospheric history of HFC-23 that was reasonably consistent with Oram et al., (1998)
94 results. Kim et al., (2010), reported HFC-23 measurements (November 2007-December 2008)
95 from Gosan, Jeju Island, South Korea and also estimated regional atmospheric emissions. Asian
96 emissions of HFC-23, including those for China have been reported by Yokouchi et al., 2006;
97 Stohl et al., 2010; Li et al., 2011; Yao et al., 2012. Most recently, Fang et al., (2014, 2015) have
98 provided bottom-up and top-down estimates of HFC-23 emissions from China and east Asia and
99 included observed HFC-23 mixing ratios at three stations - Gosan, South Korea, and Hateruma
100 and Cape Ochi-ishi, Japan. Remote sensing observations of HFC-23 in the upper troposphere
101 and lower stratosphere by two solar occultation instruments have also been reported (Harrison et
102 al., 2012), indicating an abundance growth rate of $5.8 \pm 0.3\%$ per year, similar to the CGAA
103 surface trend of $5.7 \pm 0.4\%$ per year over the same period (1989-2007).

104 HCFC-22 is used principally in air-conditioning and refrigeration, with minor uses in
105 foam blowing and as a chemical feedstock in the manufacture of fluoropolymers, such as
106 polytetrafluorethylene (PTFE). HCFC-22 production and consumption (excluding feedstock use)
107 are controlled under the Montreal Protocol. We have previously reported on the changing trends
108 and emissions of HCFC-22 (Simmonds et al., 2017 and references therein).

109 Technical solutions to mitigate HFC-23 emissions have included optimisation of the
110 HCFC-22 production process and voluntary and regulatory capture and incineration in
111 developed (Annex 1) countries (McCulloch, 2004). Mitigation in developing countries (Non-

112 Annex 1) has been introduced under the United Nations Framework Convention on Climate
113 Change (UNFCCC) Clean Development Mechanism (CDM) to destroy HFC-23 from HCFC-22
114 production facilities (UNEP, 2017a). This allowed certain HCFC-22 production plants in
115 developing countries to be eligible to provide Certified Emission Reduction (CER) credits for
116 the destruction of the co-produced HFC-23. Beginning in 2003, there were 19 registered HFC-23
117 incineration projects in five developing countries with the number of projects in each country
118 shown in parenthesis: China (11), India (5), Korea (1), Mexico (1) and Argentina (1) (Miller et
119 al., 2010). The first CER credits under the CDM for HFC-23 abatement in HCFC-22 plants were
120 approved in 2003 with funding through 2009. However, the CDM projects covered only about
121 half of the HCFC-22 production in developing countries. The substantial reduction in global
122 HFC-23 emissions during 2007-2009 was attributed by Miller et al. (2010) to the destruction of
123 HFC-23 by CDM projects. In a subsequent paper, Miller and Kuijpers (2011) predicted future
124 increases in HFC-23 emissions by considering three scenarios: a reference case with no
125 additional abatement, and two opposing abatement measures, less mitigation and best practice
126 involving increasing application of mitigation through HFC-23 incineration. Historically there
127 has been a lack of information about HFC-23 emissions from the non-CDM HCFC-22
128 production plants, although Fang et al. (2015) provided a top-down estimate of HFC-23/HCFC-
129 22 co-production ratios in non-CDM production plants. They reported that the HFC-23/HCFC-
130 22 co-production ratios in all HCFC-22 production plants were $2.7\% \pm 0.4$ by mass in 2007,
131 consistent with values reported to the Executive Committee of the Montreal Protocol (UNEP,
132 2017a).

133 Here, we use the high frequency atmospheric observations of HFC-23 and HCFC-22
134 abundances measured by (GC-MS) at the five longest-running remote sites of the Advanced
135 Global Atmospheric Gases Experiment (AGAGE). The site coordinates and measurement time
136 frames of HFC-23 and HCFC-22 are listed in Table 1. To extend our understanding of the long-
137 term growth rate of HFC-23, we combine the direct AGAGE atmospheric observations with
138 results from an analysis of firm air collected in Antarctica and Greenland, a series of old
139 Northern Hemisphere air samples, and archived air from the CGAA (Fraser et al. (1991). The
140 AGAGE 2-D 12-box model and a Bayesian inversion technique are used to produce global
141 emission estimates for HFC-23 and HCFC-22 (Cunnold et al., 1983; Rigby et al., 2011, 2014).
142 We also include observations from the AGAGE Jungfraujoch station to determine estimates of
143 European HFC-23 emissions (see section 3.3).

144
145
146

147 2. Methodology

148 2.1. AGAGE Instrumentation and Measurement Techniques

149 Ambient air measurements of HFC-23 and HCFC-22 at each site are made using the
150 AGAGE GC-MS-Medusa instrument which employs an adsorbent-filled (HayeSep D) microtrap
151 cooled to $\sim -175^{\circ}\text{C}$ to pre-concentrate the analytes during sample collection from 2 litres of air
152 (Miller et al., 2008; Arnold et al., 2012). Samples are analysed approximately every 2 hours and
153 are bracketed by measurements of quaternary standards to correct for short-term drifts in
154 instrument response. Additional details of the analytical methodology are provided in the
155 Supplementary material (1).

156 2.2. Firn and Archived Air

157 We used air samples from firn and archived in canisters to reconstruct an atmospheric
158 HFC-23 history. Firn air samples from Antarctica and Greenland were analysed for HFC-23
159 using the same technology as the *in situ* measurements; details are provided in the
160 Supplementary Material (2). The Antarctic samples were collected at the DSSW20K Law Dome
161 site in 1997-1998 (Trudinger et al., 2002) and include one deep sample from the South Pole
162 collected in 2001 (Butler et al., 2001). Greenland samples were collected at the NEEM (North
163 Greenland Eemian Ice Drilling) site in 2008 (Buizert et al., 2012). The CSIRO firn model
164 (Trudinger et al., 1997, 2013) was used to derive age spectra for the individual firn samples and
165 more details on these samples and their analysis are given in Vollmer et al. (2016, 2018) and
166 Trudinger et al. (2016). A diffusion coefficient of HFC-23 relative to CO_2 of 0.797 was used
167 (Fuller et al., 1966).

168 CGAA measurements from three separate analysis periods were also used for the
169 reconstruction of past HFC-23 abundances. The CGAA samples have been collected since 1978
170 at the Cape Grim Air Pollution Station and amount to >130 samples, the majority in internally
171 electropolished stainless steel canisters (Fraser et al., 2016, 2017). Samples were analysed under
172 varying conditions in 2006, 2011 and 2016. Here, we use a composite of the results from these
173 measurement sets. Details are given in the Supplementary Material (2) and by Vollmer et al.
174 (2018). A series of old Northern Hemisphere (NH) air samples were also measured together with
175 the measurements of the CGAA samples at the Scripps Institution of Oceanography see
176 Supplementary Material (2) and Mühle et al., (2010; Vollmer et al., (2016).

177 2.3. Calibration Scales

178 The estimated accuracies of the calibration scales for HFC-23 and HCFC-22 are
179 discussed below and a more detailed discussion of the measurement techniques and calibration

180 procedures are reported elsewhere (Miller et al., 2008; O'Doherty et al., 2009; Mühle et al.,
181 2010). HFC-23 and HCFC-22 measurements from all AGAGE sites are reported relative to
182 the SIO-07 and SIO-05 primary calibration scales respectively, which are defined by suites of
183 standard gases prepared by diluting gravimetrically prepared analyte mixtures in N₂O to near-
184 ambient levels in synthetic air (Prinn et al., 2000; Miller et al., 2008).

185 The absolute accuracies of these primary standard scales are uncertain because possible
186 systematic effects are difficult to quantify or even identify. Combining known statistical and
187 estimated systematic uncertainties, such as measurement and propagation errors, and quoted
188 reagent purities, generally yields lower uncertainties than are supported by comparisons among
189 independent calibration scales (Hall et al., 2014). Furthermore, some systematic uncertainties
190 may be normally distributed, while others, like reagent purity, are skewed in one direction.
191 Estimates of calibration accuracies and their uncertainties are nevertheless needed for
192 interpretive modelling applications. So, despite the difficulty in estimating unknown
193 uncertainties, it is incumbent on those responsible for the measurements to provide an overall
194 assessment of accuracy. Accordingly, we liberally estimate the absolute accuracies of these
195 measurements as -3% to +2% for HFC-23 and $\pm 1\%$ for HCFC-22. The larger and asymmetric
196 uncertainty for HFC-23 is due to its lower atmospheric and standard concentration, and to the
197 lower stated purity of the HFC-23 reagent used to prepare the primary calibration scale.

198

199 2.4. Selection of baseline data (unpolluted background air)

200 Baseline *in situ* monthly mean HFC-23 and HCFC-22 mole fractions were calculated by
201 excluding values enhanced by local and regional pollution influences, as identified by the
202 iterative AGAGE pollution identification algorithm (for details, see Appendix in O'Doherty et
203 al., 2001). Briefly, baseline measurements are assumed to have Gaussian distributions around the
204 local baseline value, and an iterative process is used to filter out the data that do not conform to
205 this distribution. A second-order polynomial is fitted to the subset of daily minima in any 121-
206 day period to provide a first estimate of the baseline and seasonal cycle. After subtracting this
207 polynomial from all the observations, a standard deviation and median are calculated for the
208 residual values over the 121-day period. Values exceeding three standard deviations above the
209 baseline are assigned as non-baseline (polluted) and removed from further consideration. The
210 process is repeated iteratively to identify and remove additional non-baseline values until the
211 new and previous calculated median values agree within 0.1%.

212

213 2.5. Bottom-up emissions estimates

214 The sources of information on production and emissions of HFCs are generally incomplete
215 and do not provide a comprehensive database of global emissions. In Supplementary Material
216 (3), we compile global HCFC-22 production and HFC-23 emissions data. HCFC-22 is used in
217 two ways: (1) dispersive applications, such as refrigeration and air conditioning, whose
218 production is controlled under the Montreal Protocol and reported by countries as part of their
219 total HCFC production statistics, and (2) feedstock applications in which HCFC-22 is a reactant
220 in chemical processes to produce other products. Although there is an obligation on countries to
221 report HCFC-22 feedstock use to UNEP, this information is not made public. HCFC-22
222 production for dispersive uses was calculated from the UNEP HCFC database (UNEP, 2017b)
223 and the Montreal Protocol Technology and Economic Assessment Panel 2006 Assessment
224 (TEAP, 2006). Production for feedstock use was estimated using trade literature as described in
225 the Supplementary Material (3) and the sum of production for dispersive and feedstock uses is
226 shown in Table S3.

227 HFC-23 emissions from Annex 1 countries are reported as a requirement of the
228 UNFCCC. Table S4 shows the total annual HFC-23 emissions reported by these countries
229 (UNFCCC, 2017). There is a small uncertainty in these UNFCCC emissions due to whether
230 countries report on a calendar or fiscal year basis. The data include emissions from use of HFC-
231 23 in applications such as semi-conductor manufacture and fire suppression systems. These
232 minor uses of HFC-23, originally produced in a HCFC-22 plant, will result in the eventual
233 emission of most or all into the atmosphere and emissions have remained relatively constant at
234 $0.13 \pm 0.01 \text{ Gg yr}^{-1}$, a maximum of 10% of all emissions (UNFCCC, 2017). Non-Annex 1
235 countries listed in Table S4 were eligible for financial support for HFC-23 destruction under the
236 CDM. Their emissions were calculated by applying factors to their estimated production of
237 HCFC-22 and offsetting this by the amount destroyed under CDM, as described in the
238 Supplementary Material (3). We discuss these independent emission estimates because they are
239 useful as *a priori* data constraints (“bottom-up” emission estimates) which we compare to
240 observation-based “top-down” estimates.

241 2.6. Global atmospheric model

242 Emissions were estimated using a Bayesian approach in which our *a priori* estimates of
243 the emissions growth rate were adjusted by comparing modelled baseline mole fractions to the
244 atmospheric observations (Rigby et al., 2011, 2014). The firm air measurements were included in
245 the inversion, with the age spectra from the firm model used to relate the firm measurements to
246 high-latitude atmospheric mole fractions (Trudinger et al., 2016; Vollmer et al., 2016). A 12-box

247 model of atmospheric transport and chemistry was used to simulate baseline mole fractions,
248 which assumed that the atmosphere was divided into four zonal bands (90-30°N, 30-0°N, 0-30°S,
249 30-90°S) and at 500hPa and 200hPa vertically (Cunnold et al., 1994; Rigby et al., 2013). The
250 model uses an annually repeating, monthly varying hydroxyl radical (OH) field from
251 Spivakovsky et al (2000), which has been adjusted to match the observed trend in methyl
252 chloroform (e.g. Rigby et al. 2013). For the gases in this paper, potential variations in OH
253 concentration (e.g. Rigby et al., 2017) were not found to lead to a large change in the derived
254 emissions (see Supplementary Material 4). Annually repeating, monthly varying transport
255 parameters were used as described in Rigby et al., (2014). The temperature-dependent rate
256 constant for reaction with OH was taken from Burkholder et al. (2015), which led to a lifetime of 237
257 yr for HFC-23 and 11.6 yr for HCFC-22. As in previous publications (e.g. Rigby et al., 2014),
258 uncertainties in the monthly mean baseline observations in each semi-hemisphere were taken to be the
259 quadratic sum of the measurement repeatability and the variability of the observations within the month
260 that were flagged as “baseline”, using the method in O’Doherty et al. (2001). The variability was used
261 to approximate model uncertainty, as it was assumed to be a measure of the time scales not
262 resolved by the model. No correlated uncertainties were assumed in the model-measurement mismatch
263 uncertainty and both the model-measurement mismatch and the *a priori* constraint were assumed to be
264 described by Gaussian probability density functions. Seasonal emissions estimates in each semi-
265 hemisphere were derived in the inversion. The inversion propagates uncertainty estimates from the
266 measurements, model and prior emissions growth rate to these *a posteriori* emissions estimates. The prior
267 emissions growth rate uncertainty was somewhat arbitrarily chosen at a level of 20% of the maximum *a*
268 *priori* emissions and no correlation was assumed between prior estimates of annual emissions growth
269 rate. In contrast to Rigby et al. (2014), in which a scaling factor of the emissions was solved for in the
270 inversion, here we determined absolute emissions, which were found to lead to more robust uncertainty
271 estimates when emissions were very low. *A posteriori* emissions uncertainties were augmented with an
272 estimate of the influence of uncertainties in the lifetime, as described in Rigby et al. (2014).

273

274 2.7. Regional scale atmospheric inversion

275 HFC-23 pollution events are still observed at sites in north east Asia and Europe. The
276 former have recently been used in regional scale inverse modelling studies to derive emission
277 estimates for the Asian region and these results are summarised in Section 3.3. In contrast, little
278 attention has recently been given to HFC-23 emissions from Europe. We examine European
279 emissions, using a regional scale inversion tool based on source sensitivities as estimated by a
280 Lagrangian Particle Dispersion Model run in backward mode, combined with a Bayesian
281 inversion framework.

282

283 2.7.1. Transport simulations

284 Surface source sensitivities were computed with the Lagrangian Particle Dispersion
285 Model (LPDM) FLEXPART (Stohl et al., 2005) driven by operational analysis/forecasts from
286 the European Centre for Medium-Range Weather Forecasts (ECMWF) Integrated Forecasting
287 System (IFS) modelling system with a horizontal resolution of $0.2^\circ \times 0.2^\circ$ for central Europe and
288 $1^\circ \times 1^\circ$ elsewhere. 50,000 model particles were released for each 3-hourly time interval and
289 followed backward in time for 10 days.

290

291 2.7.2. Bayesian inversion framework

292 A spatially resolved, regional-scale emission inversion, using the FLEXPART-derived
293 source sensitivities and a Bayesian approach was applied to estimate European HFC-23 annual
294 emissions for individual years between 2009 and 2016. The details of the inversion method were
295 recently published in estimating Swiss methane emissions (Henne et al., 2016). This inversion
296 methodology was part of an HFC inversion inter-comparison (Brunner et al, 2017) and was
297 applied to HFC and HCFC emissions in the eastern Mediterranean (Schönenberger et al., 2017).
298 Here, the inversion relies on the continuous observations from the Jungfrauoch and Mace Head
299 and requires *a priori* estimates of the emissions distribution. The observations are split into a
300 baseline concentration and above-baseline excursions of the signal that are attributed to recent
301 emissions using the method of Ruckstuhl et al. (2012). The inversion estimates spatially
302 distributed, annual mean emissions and a two-weekly concentration baseline. In the case of
303 HFC-23 the baseline concentration is very well defined due to the relatively infrequent
304 occurrence of larger pollution events. The inversion results were not significantly different when
305 the baseline was not updated as part of the inversion. The spatial distribution was solved on a
306 grid with different sized rectangular cells. The grid size was inversely proportional to annual
307 total source sensitivities and, therefore, was finer close to the measurement sites and coarser in
308 more remote regions that seldom influence the sites. In contrast to previous applications, the grid
309 resolution was also increased around likely point emitters in order to better localise these
310 potentially large contributors.

311 In this study the inversion was set up using complete covariance matrices. We designed
312 the *a priori* covariance matrix in such a way that the total *a priori* uncertainty for each of the
313 regions/countries was 200% and proportional to the emissions in each inversion grid cell. Off-
314 diagonal elements of the matrix were filled with the assumption of exponentially decaying
315 spatial correlation of the uncertainties with a length scale of 10 km. The choice of this rather

316 small spatial correlation scale was motivated by the assumed strong contribution from point
317 source emissions, which should result in spatially rather uncorrelated *a priori* uncertainties.
318 The data-mismatch covariance matrix contained uncertainty elements that describe the
319 uncertainty of the observations and the transport model. The observation uncertainty was taken
320 from target gas measurements, whereas the model uncertainty was estimated as the RMSE (root
321 mean square) of the *a priori* simulations Henne et al., (2016). The off-diagonal elements of the
322 covariance matrix were again assumed to exponentially decay with time between the data points.
323 The resulting correlation time scale was estimated separately for each site from a fit to the auto-
324 correlation function of the prior model residuals (see Schönerberger et al., 2017) and was in the
325 order of 0.2 to 0.3 days.

326

327 2.7.3. *A priori* emissions and sensitivity inversions

328 Spatially distributed *a priori* emissions were generated from individual national inventory
329 reports (NIR) to UNFCCC (2017). Most European countries separately list the emissions of
330 HFC-23 by sector in Table 2(II) of their submissions. Here, we chose two different approaches
331 to spatially distribute these bottom-up estimates and use these as input for two sensitivity
332 inversions. In the first approach (UNFCCC_org), we directly follow the categorisation in each
333 NIR and assign emissions from ‘Fluorochemical production’ to individual production sites as
334 taken from Keller et al. (2011), and shown in Figure S4, whereas emissions from ‘Electronics
335 industry’ and ‘Product use’ were distributed according to population density (Center for
336 International Earth Science Information Network - CIESIN - Columbia University. 2016,
337 available at <https://ciesin.columbia.edu/data/hrsl/>). Countries reporting no or zero HFC-23
338 emissions were assigned a *per capita* emission factor equal to 1/10 of the average *per capita*
339 emission factor from reporting countries. This mostly impacts countries at the periphery of the
340 inversion domain. In our second approach (UNFCCC_r0.5), we used the same spatial
341 disaggregation as before, but assigning 50% of the ‘Electronics industry’ and ‘Product use’
342 emissions in each country to the likely point source locations and distribute the remainder by
343 population. Inversions using the HFC-23 inventory provided by EDGAR (version 4.2) as *a*
344 *priori* were tested. However, these inversions showed much weaker model performance than
345 those based on UNFCCC priors and, hence, were dropped from any further analysis.

346

347

348

349 3. Results and Discussion

350 3.1. Atmospheric mole fractions

351 Figure 1 shows the HFC-23 modelled mole fraction for the four equal-mass latitudinal
352 subdivisions of the global atmosphere calculated from the 12-box model and the combined GC-
353 MS-Medusa *in situ* measurements (2008-2016), firm air data, old NH air and CGAA data. The
354 lower box shows the annual growth rates in $\text{pmol mol}^{-1} \text{yr}^{-1}$. We find that the global modelled
355 annual mole fraction of HFC-23 in the background atmosphere reached $28.9 \pm 0.6 \text{ pmol mol}^{-1}$,
356 (1σ confidence interval) in December 2016, a 163% increase from 1995 and a 28% increase
357 from the $22.6 \pm 0.2 \text{ pmol mol}^{-1}$ reported in 2009 (Miller et al., 2010). In 2008 the annual mean
358 mid-year growth rate of HFC-23 was $0.78 \text{ pmol mol}^{-1} \text{yr}^{-1}$. By mid-2009 the growth rate
359 decreased to $0.68 \text{ pmol mol}^{-1} \text{yr}^{-1}$, rising to a maximum of $1.05 \text{ pmol mol}^{-1} \text{yr}^{-1}$ in early 2014,
360 followed by a smaller decrease to $0.95 \text{ pmol mol}^{-1} \text{yr}^{-1}$ in 2016. The growth rate of HFC-23
361 increased by 22 % from 2008 to 2016. In the Figure 1 inset, we compare the annual mean mole
362 fractions of HFC-23 and HCFC-22 recorded at Mace Head and Cape Grim, as examples of mid-
363 latitude northern hemisphere (NH) and southern hemisphere (SH) sites, illustrating the site
364 divergence for these two compounds beginning around 2010.

365 Figure 2 shows our HCFC-22 modelled mole fractions for the four equal-mass latitudinal
366 subdivisions of the global atmosphere calculated from the 12-box model and the lower box
367 shows the HCFC-22 annual growth rates in $\text{pmol mol}^{-1} \text{yr}^{-1}$. The global modelled HCFC-22
368 annual mixing ratio in the background atmosphere reached peaked at $238 \pm 2 \text{ pmol mol}^{-1}$ in
369 December 2016, following the decline in the annual average global growth rate of HCFC-22
370 from 2008 to 2016 of $0.5 \text{ pmol mol}^{-1} \text{yr}^{-2}$. This decline in the global growth rate of HCFC-22
371 coincides with the phase out of HCFC production/consumption mandated by the 2007
372 amendment to the Montreal Protocol for Annex 1 countries, covering dispersive applications, but
373 not the non-dispersive use of HCFC-22 as a feedstock in fluoropolymer manufacture (UNEP,
374 2017a). Nevertheless, HCFC-22 remains the dominant HCFC in the atmosphere and accounts for
375 79% by mass of the total global HCFC emissions (Simmonds et al., 2017). In contrast to the
376 increasing growth rate of HFC-23, the growth rate of HCFC-22 has exhibited a steep 53%
377 decline from a maximum in January 2008 of $8.2 \text{ pmol mol}^{-1} \text{yr}^{-1}$ to $3.8 \text{ pmol mol}^{-1} \text{yr}^{-1}$ in
378 December 2016, further illustrating the divergence between these two gases between 2008 and
379 2016 (compare lower boxes in Figures 1 and 2). These results are an update of our previously
380 reported analysis AGAGE HCFC-22 data (Simmonds et al., 2017) for the period 1995-2015.

381

382

383 3.2. Global emission estimates

384 Miller et al. (2010) calculated global emissions of HFC-23 using the same AGAGE 12-
385 box model as used here, but with a different Bayesian inverse modelling framework. Following a
386 peak in emissions in 2006 of $15.9 (+1.3/-1.2)$ Gg yr⁻¹, modelled emission estimates of HFC-23
387 declined rapidly to $8.6 (+0.9/-1.0)$ Gg yr⁻¹ in 2009, which Miller noted was the lowest annual
388 emission for the previous 15 years. Based on the analysis of firm air samples and ambient air
389 measurements from Antarctica, Montzka et al. (2010) reported global HFC-23 emissions of 13.5
390 ± 2 Gg yr⁻¹ (200 ± 30 Mt CO₂-e yr⁻¹), averaged over 2006-2008. In Carpenter and Reimann
391 (2014), global emissions of HFC-23 estimated from measured and derived atmospheric trends
392 reached a maximum of 15 Gg yr⁻¹ in 2006, declined to 8.6 Gg in 2009, and subsequently
393 increased again to 12.8 Gg in 2012 (Figure 1-25, update of Miller et al., 2010 and Montzka et al.,
394 2010).

395 The model derived HFC-23 emissions from this study, shown in Figure 3 and listed in
396 Table 2, reached an initial maximum in 2006 of 13.3 ± 0.8 Gg yr⁻¹, then declined steeply to $9.6 \pm$
397 0.6 Gg yr⁻¹ in 2009. Our HFC-23 emissions estimates, which include firm data and NH archive
398 air samples and a slightly different inverse method, are slightly lower in 2006 and slightly higher
399 in 2009 than the HFC-23 estimates of Miller et al. (2010) and Carpenter and Reimann (2014)
400 respectively. Our mean annual (2006-2008) HFC-23 emissions of $12.1 (\pm 0.7)$ Gg yr⁻¹ are lower
401 than the Montzka et al., (2010) emissions estimates of 13.5 ± 2 Gg yr⁻¹, but agree within
402 uncertainties. However, our HFC-23 emissions then grew rapidly reaching a new maximum of
403 14.5 ± 0.6 Gg yr⁻¹ (180 ± 7 Mt CO₂-eq yr⁻¹) in 2014, only to decline again to 12.7 ± 0.6 Gg yr⁻¹
404 (157 ± 7 Mt CO₂-eq yr⁻¹) in 2016. Cumulative HFC-23 emissions estimates from 2010 to 2016
405 were 89 ± 16 Gg (1.1 ± 0.2 Gt CO₂-e), contributing to an increase in radiative forcing of $1.0 \pm$
406 0.1 mW m⁻².

407 The global emission estimates for HCFC-22 are plotted in Figure 4 together with the
408 corresponding Miller et al. (2010) emissions up to 2008 and the WMO 2014 emissions estimates
409 (Carpenter and Reimann, 2014). Table 3 lists the global emission estimates, mole fractions and
410 growth rate of HCFC-22. Our modelled HCFC-22 emissions reached a maximum global
411 maximum of 385 ± 41 Gg yr⁻¹ (696 ± 74 Mt CO₂-eq yr⁻¹) in 2010, followed by a slight decline to
412 370 ± 46 Gg yr⁻¹ (670 ± 83 Mt CO₂-eq yr⁻¹) in 2016 at an annual average rate of 2.3 Gg yr⁻¹.

413 3.3. Regional emissions

414 Several papers report Asian emissions of HFC-23, including those for China (Yokouchi et
415 al., 2006; Stohl et al., 2010; Kim et al., 2010; Li et al., 2011; Yao et al., 2012). Recent papers by
416 Fang et al. (2014, 2015) noted inconsistencies between the various bottom-up and top-down

417 emissions estimates and provided an improved bottom-up inventory and a multi-annual top-
418 down estimate of HFC-23 emissions for east Asia. They showed that China contributed 94-98 %
419 of all HFC-23 emissions in east Asia and was the dominant contributor to global emissions: $20 \pm$
420 6 % in 2000 rising to 77 ± 23 % in 2005. China's annual HFC-23 top-down emissions in 2012
421 were estimated at 8.8 ± 0.8 Gg yr⁻¹ (Fang et al., 2015), 69% of our 2012 global emissions
422 estimate of 12.9 ± 0.6 Gg yr⁻¹, listed in Table 2.

423 Based on the bottom-up estimated global HFC-23 emissions (shown in Supplementary
424 Material (3), Table S4), we show in Figure 5a global and Chinese emissions and the percentage
425 of Chinese emissions contributing to the global total. These bottom-up estimates show that a
426 steadily increasing fraction of global total HFC-23 emissions can be attributed to China,
427 averaging about 88% in 2011-2014. This rise is consistent with the increase in our calculated
428 bottom-up HCFC-22 production data compiled from industry sources and listed in
429 Supplementary Material (3), Table S3. Figure 5b, shows the bottom-up estimates of global and
430 China HCFC-22 production and the percentage contribution of China production to the global
431 total, further illustrating the dominance of HCFC-22 production in China.

432 Clearly China is the major contributor to recent global HFC-23 emissions which implies only
433 minor contributions from other regional emitters. However, HFC-23 pollution events are still
434 observed at our European sites. Keller et al. (2011) reported European HFC-23 emissions based
435 on inverse modelling for the period summer 2008 to summer 2010, assigning most of the
436 emissions to point sources at HCFC-22 production sites. Here, we re-evaluated European HFC-
437 23 emissions for the period 2009 to 2016 (see section 2.7). The key results from this analysis are
438 summarised in Figures 6 and in Table 4 and more detailed results are available in the
439 Supplementary Material (5).

440 Based on these inversion results, European emissions of HFC-23, though small on a
441 global scale were, in general, larger than reported to UNFCCC and exhibited considerable year-
442 to-year variability (Table 4, Figure 6 and spatial distribution Figure S4). Total *a posteriori*
443 emissions for the six European regions reached a maximum of 0.30 ± 0.05 Gg yr⁻¹ in 2013
444 declining to 0.17 ± 0.03 Gg yr⁻¹ in 2016 and showed a slightly negative, statistically insignificant
445 trend over the period analysed (2009-2016). The cumulative European HFC-23 emissions from
446 2010-2016 were ~1.3 Gg corresponding to just 1.5% of our cumulative global HFC-23
447 emissions over this same period of 89 Gg (Table 2). Considerable differences between the two
448 inversions with different *a priori* emission distributions (see section 2.7.3) were observed on a
449 country scale, with generally larger Italian *a posteriori* emissions when the original UNFCCC
450 split of point and area sources was used in the *a priori* (UNFCCC_org). In this case the inversion

451 was not able to completely relocate the area emissions, but at the same time increased emissions
452 at the point source locations and resulting in overall larger *a posteriori* emissions. For both
453 sensitivity inversions the fraction of European emissions within grid boxes containing HCFC-22
454 production facilities, increased in the *a posteriori* as compared with the *a priori* distribution
455 (Table 4 and Figure S4).

456 In the following section we attempt to reconcile the changing trends in global HFC-23
457 emissions with the decrease in global HCFC-22 emissions after 2010 and the decline in the
458 annual HCFC-22 growth rate. There are a number of key factors which we believe can explain
459 the changing trend in the recent history of HFC-23 emissions after the minimum in 2009.

460 3.4. Factors affecting the recent increase in HFC-23 emissions and changes in the
461 consumption of produced HCFC-22.

462 1. Recent publications have highlighted the substantial increase in HCFC-22 production in
463 Non-Annex 1 countries since the 1990s, especially in the last decade, due to increasing demand
464 in air-conditioning, refrigeration applications and primarily from the use of HCFC-22 as a
465 feedstock in fluoropolymer manufacture (UNEP, 2009; Miller et al., 2010; USEPA, 2013; Fang
466 et al., 2015). This has resulted in Non-Annex 1 countries emitting more co-produced HFC-23
467 than Annex 1 countries since about 2001 (Miller et al., 2010). HCFC-22 production in Annex 1
468 countries in 2015 had shrunk by 45% from the peak historic value of 407 Gg yr⁻¹ in 1996 (see
469 Supplementary Material (3), Table S3). This has been accomplished by plant closures and
470 further reductions of HFC-23 emissions by enhanced destruction in the remaining plants.
471 Nevertheless, ~ 1 Gg of HFC-23 was emitted in 2015 from HCFC-22 production in Annex 1
472 countries, mainly from Russia and USA (96%). For comparison, the combined HFC-23
473 emissions in 2015 from the six European regions (listed in Table 4) were just 0.11 ± 0.03 Gg.

474

475 2. Since 2006, a major factor mitigating HFC-23 emissions has been the CERs issued under
476 the CDM. However, under the original CDM rules, large CERs that cost relatively little to
477 acquire could be claimed legitimately (Munnings et al., 2016) and the rules were changed to bar
478 new entrants to the mechanism after 2009. The HFC-23/HCFC-22 co-production or waste gas
479 generation ratio varies between 1.5 - 4% (by mass) depending on HCFC-22 plant operating
480 conditions and process optimization (McCulloch and Lindley, 2007). Under the
481 UNFCCC/CDM, 19 HCFC-22 production plants in five Non-Annex 1 countries - Argentina (1),
482 China (11), Democratic People's Republic of Korea (1), India (5) and Mexico (1) - were
483 approved for participation in CDM projects. These countries reportedly incinerated 5.7 Gg and
484 6.8 Gg of HFC-23 in 2007 and 2008, respectively (UNFCCC, 2009). This represented 43 - 48%

485 of the HCFC-22 produced in Non-Annex 1 countries during 2007-2008 assuming the 1.5 - 4%
486 co-production factor (Montzka et al., 2010). These five countries produced 597 Gg of HCFC-22
487 from controlled and feed stock uses in 2015. HFC-23 generated from this HCFC-22 production
488 was estimated at 16 Gg with an average co-production ratio of 2.6%. Furthermore, it was
489 estimated that China produced 535 Gg of HCFC-22 in 2015 (~90% of the five countries' total
490 production) and 45% of the co-produced HFC-23 generated was destroyed in the CDM
491 destruction facilities (UNEP, 2017a). The first seven-year crediting period of CDM projects in
492 China expired in 2013, concurrent with the European Union ceasing the purchase of CER credits
493 for HFC-23 produced in industrial processes after May 2013 (Fang et al., 2014).

494

495 3. Lastly, we should consider whether there are other sources of HFC-23 which might
496 explain an increase in global emissions. While the major source of all HFC-23 is HCFC-22 co-
497 production, material that is recovered and sold may subsequently be emitted to the atmosphere.
498 Emissions of HFC-23 from fire suppression systems are negligible relative to global production
499 (McCulloch and Lindley, 2007) and emissions from all emissive uses are reported to be $0.13 \pm$
500 0.01 Gg yr⁻¹ from Annex 1 countries (UNFCCC, 2017) and less than 0.003 Gg for the
501 refrigeration and fire-fighting sectors in 2015 in the five Non-Annex 1 countries listed above,
502 (UNEP, 2017a). Semi-conductor use of HFC-23 is insignificant having been replaced by more
503 efficient etchants and where destruction efficiencies are greater than 90% (Bartos et al., 2006,
504 Miller et al., 2010). Fraser et al. (2013) reported a very small emissions factor of 0.04 g HFC-23
505 Mg⁻¹ aluminium (Al) from the Kurri Kurri smelter in NSW, Australia. It was estimated that this
506 corresponds to an annual emission of HFC-23 from Al production of ~0.003 Gg based on a
507 global Al production of 57 Tg in 2016 (<http://www.world-aluminium.org/statistics/#data>,
508 accessed 2016). Realistically, these other potential industrial sources of HFC-23 emissions are
509 very small (< 0.015 Gg yr⁻¹) in the context of global emissions estimates.

510 The combination of these factors strongly suggests that the steep reversal of the
511 downwards trend in HFC-23 emissions after 2009 is attributable to HFC-23 abatement measures
512 not being adequate to offset the increasing growth in production of HCFC-22 for non-dispersive
513 feedstock. This is despite the initial success of CDM abatement technologies leading to
514 mitigation of HFC-23 emissions during 2006-2009.

515 **4. Conclusions**

516 The introduction of CERs under the CDM did contribute to a reduction of HFC-23
517 emissions in Non-Annex 1 countries during 2006-2009, thereby lowering global emissions,
518 reaching a minimum of 9.6 ± 0.6 Gg yr⁻¹ in 2009. However, from 2010 to 2014 global HFC-23

519 emissions increased steadily at an annual average rate of ~ 1 Gg yr⁻¹ reaching a new maximum of
520 14.5 ± 0.6 Gg yr⁻¹ in 2014. This period coincides with the highest levels of our bottom-up
521 estimates of HCFC-22 production in Non-Annex 1 countries (Supplementary Material (3), Table
522 S3), coinciding with a transition period when HCFC-22 production plants without any abatement
523 controls had yet to install incineration technologies or fully adopt process optimisation
524 techniques. Furthermore, non-CDM plants are not required to report co-produced HFC-23
525 emissions, although Fang et al. (2015) calculated that these plants have a lower HFC-23/HCFC-
526 22 production ratio as they came into operation after the CDM period and would most likely be
527 using improved technologies for HFC-23 abatement.

528 Our cumulative HFC-23 emissions estimates from 2010 to 2016 were 89.1 ± 4.3 Gg (1.1 ± 0.2
529 Gt CO₂-eq), which led to an increase in radiative forcing of 1.0 ± 0.1 mW m⁻². This implies that
530 the post-2009 increase in HFC-23 emissions resulted from the decision not to award new CDM
531 projects after 2009, against a background of increasing production of HCFC-22 in plants that did
532 not have abatement technology. Over this same time frame, the magnitude of the cumulative
533 emissions of HCFC-22 was 2610 ± 311 Gg (4724 Mt CO₂-eq yr⁻¹). During 2015-2016 our results
534 show a decline of about 9% in average global HFC-23 emissions (12.9 Gg yr⁻¹) relative to the
535 2013-2014 average of 14.2 Gg yr⁻¹. We note that in the Kigali 2016 Amendment to the Montreal
536 Protocol, China committed to a domestic dispersive HCFC-22 production reduction of 10% by
537 2015 compared to the average 2009-2010 production (UNEP, 2017a). While this regulation
538 should decrease HCFC-22 production for dispersive uses, overall HFC-23 emissions could still
539 continue to increase due to a potential increase in the production of HCFC-22 for feedstock uses
540 (Fang et al., 2014). It is perhaps encouraging that the Kigali Amendment also stipulates that the
541 Parties to the Montreal Protocol shall ensure that HFC-23 emissions generated from production
542 facilities producing HCFCs or HFCs are destroyed to the maximum extent possible using
543 technology yet to be approved by the Parties. In 2014, with the support of the Chinese
544 Government, 13 new destruction facilities at 15 HCFC-22 production lines not covered by
545 CDM, were installed (UNEP, 2017a). The time frame of these new initiatives is consistent with
546 the most recent reduction (2015-2016) of global HFC-23 emissions.

547 The mismatch between mitigation and emissions, that is most evident in China, suggests
548 that the delay in the implementation of additional abatement measures allowed HFC-23
549 emissions to increase before these measures became effective. Our results imply that HFC-23
550 emissions into the atmosphere will continue to increase and make a contribution to radiative
551 forcing of HFCs until the implementation of abatement becomes a universal requirement.

552

553

554 **Acknowledgements**

555 We specifically acknowledge the cooperation and efforts of the station operators (G.
556 Spain, Mace Head, Ireland; R. Dickau, Trinidad Head, California; P. Sealy, Ragged Point,
557 Barbados; NOAA Officer-in-Charge, Cape Matatula, American Samoa; S. Cleland, Cape Grim,
558 Tasmania) and their staff at all the AGAGE stations. The operation of the AGAGE stations was
559 supported by the National Aeronautics and Space Administration (NASA, USA) (grants NAG5-
560 12669, NNX07AE89G, NNX11AF17G and NNX16AC98G to MIT; grants NAG5-4023,
561 NNX07AE87G, NNX07AF09G, NNX11AF15G, NNX11AF16G, NNX16AC96G and
562 NNX16A97G to SIO). We acknowledge the Department for Business, Energy and Industrial
563 Strategy (BEIS, UK) for contract 1028/06/2015 to the University of Bristol and the UK
564 Meteorological Office in support of Mace Head, Ireland, and modelling activities; the National
565 Oceanic and Atmospheric Administration (NOAA, USA), contract RA-133-R15-CN-0008 to the
566 University of Bristol in support of Ragged Point, Barbados; we acknowledge NOAA support for
567 the operations of the American Samoa station, and support by the Commonwealth Scientific and
568 Industrial Research Organisation (CSIRO, Australia), the Bureau of Meteorology (Australia) and
569 Refrigerant Reclaim Australia for Cape Grim operations.

570 CSIRO's contribution was supported in part by the Australian Climate Change Science
571 Program (ACCSP), an Australian Government Initiative. Australian firm activities in the
572 Antarctic are specifically supported by the Australian Antarctic Science Program. We
573 acknowledge the members of the firm air sampling teams for provision of the samples from Law
574 Dome, NEEM, and South Pole. NEEM is directed and organized by the Centre of Ice and
575 Climate at the Niels Bohr Institute and US NSF, Office of Polar Programs. It is supported by
576 funding agencies and institutions in Belgium (FNRS-CFB and FWO), Canada (NRCan/GSC),
577 China (CAS), Denmark (FIST), France (IPEV, CNRS/INSU, CEA, and ANR), Germany (AWI),
578 Iceland (RannIs), Japan (NIPR), Korea (KOPRI), the Netherlands (NWO/ALW), Sweden (VR),
579 Switzerland (SNF), United Kingdom (NERC), and the U.S. (U.S. NSF, Office of Polar
580 Programs). Financial support for the Jungfraujoch measurements is acknowledged from the
581 Swiss national programme HALCLIM (Swiss Federal Office for the Environment (FOEN)).
582 Support for the Jungfraujoch station was provided by International Foundation High Altitude
583 Research Stations Jungfraujoch and Gornergrat (HFSJG).

584 M. Rigby is supported by a NERC Advanced Fellowship NE/I021365/1. We acknowledge the
585 cooperation of R. Langenfelds for his long-term involvement in supporting and maintaining the
586 Cape Grim Air Archive. We also thank S. Montzka and B. Hall for supplying actual datasets
587 from their publications.

588

589 **References.**

- 590 | Arnold, T., Mühle, J., Salameh, P. K., Harth, C.M., Ivy, D. J., and Weiss, R. F.: Automated
591 measurement of nitrogen trifluoride in ambient air, *Anal. Chem.*, 84, 4798–4804, 2012.
- 592 Bartos, S., Beu, L. S., Burton, C. S., Fraust, C. L., Illuzzi, F., Mocella, M. T., and Raoux, S.:
593 IPCC Guidelines for National Greenhouse Inventories. Volume 3, Industrial Processes, Chapter
594 6, Electronics Industry, available at: [www.ipcc-nggip.iges.or.jp/public/2006gl/pdf/3.](http://www.ipcc-nggip.iges.or.jp/public/2006gl/pdf/3_Volume3/V3.6.Ch6_Electronics_Industry.pdf)
595 [Volume3/V3.6.Ch6_Electronics_Industry](http://www.ipcc-nggip.iges.or.jp/public/2006gl/pdf/3_Volume3/V3.6.Ch6_Electronics_Industry.pdf), pdf, 2006.
- 596 Brunner, D., Arnold, T., Henne, S., Manning, A., Thompson, R. L., Maione, M., O'Doherty, S.,
597 and Reimann, S.: Comparison of four inverse modelling systems applied to the estimation of
598 HFC-125, HFC-134a and SF₆ emissions over Europe, *Atmos. Chem. Phys.*, 17, 10651-10674,
599 <https://doi.org/10.5194/acp-17-10674-2017>, 2017.
- 600 Burkholder, J. B., Sander, S. P., Abbatt, J., Barker, R., Huie, R. E., Kolb, C. E., Kurylo, M. J.,
601 Orkin, V. L., Wilmouth, D. M., and Wine, P.H.: Chemical kinetics and photochemical data for
602 use in atmospheric studies, Evaluation No. 18, JPL Publication 15-10, Jet Propul. Lab.,
603 Pasadena, Calif, 2015. [available at <http://jpldataeval.jpl.nasa.gov/>.]
- 604 Buizert, C., Martinerie, P., Petrenko, V. V., Severinghaus, J. P., Trudinger, C. M., Witrant, E.,
605 Rosen, J. L., Orsi, A. J., Rubino, M., Etheridge, D. M., Steele, L. P., Hogan, C., Laube, J. C.,
606 Sturges, W. T., Levchenko, V. A., Smith, A. M., Levin, I., Conway, T. J., Dlugokencky, E. J.,
607 Lang, P. M., Kawamura, K., Jenk, T. M., White, J. W. C., Sowers, T., Schwander, J., and
608 Blunier, T.: Gas transport in firn: multiple-tracer characterisation and model intercomparison for
609 NEEM, Northern Greenland, *Atmos. Chem. Phys.*, 12, 4259–4277, doi:10.5194/acp-12-4259-
610 2012.
- 611 Butler, J. H., Montzka, S. A., Battle, M., Clarke, A. D., Mondeel, D. J., Lind, J. A., Hall, B. D.,
612 and Elkins, J. W.: Collection and analysis of firn air from the South Pole, 2001, AGU Fall
613 Meeting Abstracts, p. F145, 2001.
- 614 Carpenter, L. J. and Reimann, S.: Ozone-Depleting Substances (ODSs) and Other Gases of
615 Interest to the Montreal Protocol, Chapter 1, in: Scientific Assessment of Ozone Depletion:
616 2014, Global Ozone Research and Monitoring Project - Report No. 55, World Meteorological
617 Organisation, Geneva, Switzerland, 2014.
- 618 Culberston, J. A., Prins, J. M., Grimsrud, E. P., Rasmussen, R.A., Khalil, M. A. K., and Shearer,
619 M. J.: Observed trends in CF₃-containing compounds in background air at Cape Meares,
620 Oregon, Point Barrow, Alaska, and Palmer Station, Antarctica, *Chemosphere*, 55, 1109–1119,
621 2004.
- 622
- 623 Cunnold, D. M., Prinn, R.G., Rasmussen, R., Simmonds, P. G., Alyea, F. N., Cardlino, C.,
624 Crawford, A. J., Fraser, P. J., Rosen, R.: The Atmospheric Lifetime Experiment, III: lifetime
625 methodology and application to three years of CFC₁₃ data, *J. Geophys. Res.*, 88, 8379-8400,
626 1983.
- 627 Cunnold, D. M., Fraser, P. J., Weiss, R. F., Prinn, R. G., Simmonds, P. G., Miller, B. R., Alyea,
628 F. N., Crawford, A. J., and Rosen, R.: Global trends and annual releases of CCl₃F and CCl₂F₂

629 estimated from ALE/GAGE and other measurements from July 1978 to June 1991, *J. Geophys.*
630 *Res.*, 99, 1107-1126, 1994.

631 Fang, X., Miller, B. R., Su, S., Wu, J., Zhang, J., and Hu, J.: Historical emissions of HFC-23
632 (CHF₃) in China and projections upon policy options by 2050, *Environ. Sci. & Technol.*, 48,
633 4056-4062, 2014.

634 Fang, X., Stohl, A., Yokouchi, Y., Kim, J., Li, S., Saito, T., Park S and Hu. J.: Multiannual top-
635 down estimate of HFC-23 emissions in east Asia. *Environ. Sci. & Technol.*, 49, 4345-4353,
636 2015.

637 Fraser, P. J., Langenfelds, R.L., Derek N and Porter, L.W.: Studies in air archiving techniques,
638 in *Baseline Atmospheric Program (Australia) 1989*, S. R. Wilson and J. L. Gras (eds.),
639 Department of the Arts, Sport, the Environment, Tourism and Territories, Bureau of
640 Meteorology and CSIRO Division of Atmospheric Research, Canberra, Australia, 16-29, 1991.

641 Fraser, P., Steele, L.P., and Cooksey, M.: PFC and carbon dioxide emissions from an Australian
642 aluminium smelter using time-integrated stack sampling and GC-MS, GC-FID analysis. *Light*
643 *Metals 2013*, B. Sadler (ed.), Wiley/TMS 2013, 871-876, 2013.

644 Fraser, P. J., Steele, L.P., Pearman, G.I., Coram, S., Derek, N., Langenfelds, R.L and Krummel,
645 P.B.: Non-carbon dioxide greenhouse gases at Cape Grim: a 40 year odyssey, *Baseline*
646 *Atmospheric Program (Australia) History and Recollections*, 40th Anniversary Special Edition,
647 Derek, N., P. B. Krummel and S. J. Cleland (eds.), Bureau of Meteorology/CSIRO Oceans and
648 Atmosphere, ISSN 0155-6959, 45-76, 2016.

649 Fraser, P. J., Pearman, G and Derek, N., I. CSIRO non-carbon dioxide greenhouse gas research.
650 Part 1: 1975-1990, *Historical Records of Australian Science*, [doi.10.1071/HR17016](https://doi.org/10.1071/HR17016), 2017.

651 Fuller, E. N., Schettler, P. D., and Giddings, J. C.: A new method for prediction of binary gas-
652 phase diffusion coefficients, *Ind. Eng. Chem.*, 30, 19-27, 1966.

653 Hall, B.D., Engel, A., Mühle, J., Elkins, J. W., Artuso, F., Atlas, E., Aydin, M., Blake, D.,
654 Brunke, E.-G., Chiavarini, S., Fraser, P. J., Happell, J., Krummel, P. B., Levin, I., Loewenstein,
655 M., Maione, M., Montzka, S. A., O'Doherty, S., Reimann, S., Rhoderick, G., Saltzman, E. S.,
656 Scheel, H. E., Steele, L. P., Vollmer, M. K., Weiss, R. F., Worthy, D., and Yokouchi, Y. 2014.,
657 Results from the International Halocarbons in Air Comparison Experiment (IHALACE), *Atmos.*
658 *Meas. Tech.*, 72, 469-490, [doi:10.5194/amt-7-469-2014](https://doi.org/10.5194/amt-7-469-2014), 2014.

659 Harrison, J. J., Boone, C. D., Brown, A. T., Allen, N. D. C., Toon, G. C., and Bernath, P. F.:
660 First remote sensing observations of trifluoromethane (HFC-23) in the upper troposphere and
661 lower stratosphere, *J. Geophys. Res.*, 117, D05308, [doi: 10.1029/2011JD016423](https://doi.org/10.1029/2011JD016423), 2012.

662 Henne, S., Brunner, D., Oney, B., Leuenberger, M., Eugster, W., Bamberger, I., Meinhardt, F.,
663 Steinbacher, M., and Emmenegger, L.: Validation of the Swiss methane emission inventory by
664 atmospheric observations and inverse modelling, *Atmos. Chem. Phys.*, 16, 3683-3710, [doi:](https://doi.org/10.5194/acp-16-3683-2016)
665 [10.5194/acp-16-3683-2016](https://doi.org/10.5194/acp-16-3683-2016), 2016.

666 Keller, C. A., Brunner, D., Henne, S., Vollmer, M. K., O'Doherty, S., and Reimann, S.:
667 Evidence for under-reported western European emissions of the potent greenhouse gas HFC-23.
668 Geophys. Res. Lett, 38, L15808, doi: 10.1029/2011GL047976, 2011.

669 Kim, J., Li, S., Kim, K. R., Stohl, A., Mühle, J., Kim, S. K., Park, M. K., Kang, D. J., Lee, G.,
670 Harth, C. M., Salameh, P. K., and Weiss, R. F.: Regional atmospheric emissions determined
671 from measurements at Jeju Island, South Korea: halogenated compounds from China, Geophys.
672 Res. Lett, 37, doi:10.1029/2010GL043263, 2010.

673 Li, S.; Kim, J.; Kim, K. R.; Mühle, J.; Kim, S. K.; Park, M. K.; Stohl, A.; Kang, D. J.; Arnold,
674 T.; Harth, C. M.; Salameh, P. K.; Weiss, R. F.: Emissions of halogenated compounds in East
675 Asia determined from measurements at Jeju Island, Korea, Environ. Sci. Technol., 45 (13),
676 5668–5675, 2011.

677 McCulloch, A.: Incineration of HFC-23 Waste Streams for Abatement of Emissions from
678 HCFC-22 Production: A Review of Scientific, Technical and Economic Aspects, commissioned
679 by the UNFCCC secretariat to facilitate the work of the Methodologies Panel of the CDM
680 Executive Board, available online at: [http://cdm.unfccc.int/methodologies/Background](http://cdm.unfccc.int/methodologies/Background240305.pdf)
681 240305.pdf, 2004.

682 McCulloch, A., and Lindley, A. A.: Global Emissions of HFC-23 estimated to year 2015.
683 Atmos. Environ, 41, 1560-1566, 2007.

684 Miller, B. R., Weiss, R. F., Salameh, P. K., Tanhua, T., Grealley, B. R., Mühle, J., Simmonds, P,
685 G.: Medusa: A sample pre-concentration and GC-MS detector system for *in situ* measurements
686 of atmospheric trace halocarbons, hydrocarbons and sulphur compounds, Anal. Chem., 80,
687 1536-1545, 2008.

688 Miller, B. R., Rigby, M., Kuijpers, L. J. M., Krummel, P. B., Steele, L. P., Leist, M., Fraser, P.
689 J., McCulloch, A., Harth, C. M., Salameh, P.K., Mühle, J., Weiss, R. F., Prinn, R.G., Wang, R.
690 H. J., O'Doherty, S., Grealley, B. R., and Simmonds, P. G.: HFC-23 (CHF₃) emission trend
691 response to HCFC-22 (CHClF₂) production and recent HFC-23 emissions abatement measures,
692 Atmos. Chem. Phys, 10, 7875-7890, 2010.

693 Miller, B. R., and Kuijpers, L. J. M.: Projecting future HFC-23 emissions, Atmos. Chem. Phys.,
694 11, 13259-13267, doi:10.5194/acp-11-13259-2011, 2011

695 Miller, M., and Batchelor, T.: Information paper on feedstock uses of ozone-depleting
696 substances, 72 pp. [Available at [http://ec.europa.](http://ec.europa.eu/clima/policies/ozone/research/docs/feedstock_en.pdf)
697 [eu/clima/policies/ozone/research/docs/feedstock_en.pdf](http://ec.europa.eu/clima/policies/ozone/research/docs/feedstock_en.pdf).] 2012.

698 Montzka, S.A., Kuijpers, L., Battle, M. O., Aydin, M., Verhulst, K. R., Saltzman, E.S. and
699 Fahey, D. W., Recent increases in global HFC-23 emissions, Geophys. Res. Lett, 37, L02808,
700 doi:10.1029/2009GL041195, 2010.

701 Mühle, J., Ganesan, A. L., Miller, B. R., Salameh, P. K., Harth, C. M., Grealley, B. R., Rigby, M.,
702 Porter, L. W., Steele, L. P., Trudinger, C. M., Krummel, P. B., O'Doherty, S., Fraser, P. J.,
703 Simmonds, P. G., Prinn, R. G., and Weiss, R. F.: Perfluorocarbons in the global atmosphere:
704 tetrafluoromethane, hexafluoroethane, and octafluoropropane, Atmos. Chem. Phys., 10, 5145–
705 5164, doi:10.5194/acp-10-5145, 2010.

706 Munnings, C., Leard, B., and Bento, A.: The net emissions impact of HFC-23 offset projects
707 from the Clean Development Mechanism, Resources for the Future, Discussion Paper 16-01,
708 2016.

709 Myhre, G., Shindell, D., Bréon, F. M., Collins, W., Fuglestvedt, J., Huang, J., Koch, D.,
710 Lamarque, J. F., Lee, D., Mendoza, B., Nakajima, T., Robock, A., Stephens, G., Takemura, T.,
711 and Zhang, H.: Anthropogenic and Natural Radiative Forcing, Chapter 8: Climate Change 2013:
712 The Physical Science Basis. Contribution of Working Group I to the Fifth Assessment Report of
713 the Intergovernmental Panel on Climate Change [Stocker, T.F., D. Qin, G.-K. Plattner, M.
714 Tignor, S.K. Allen, J. Boschung, A. Nauels, Y. Xia, V. Bex and P.M. Midgley (eds.)].
715 Cambridge University Press, Cambridge, United Kingdom and New York, NY, USA, 659-740,
716 2013.

717 O’Doherty, S., Cunnold, D., Sturrock, G. A., Ryall, D., Derwent, R. G., Wang, R. H. J.,
718 Simmonds, P. G., Fraser, P. J., Weiss, R. F., Salameh, P. K., Miller, B. R., Prinn, R. G.: *In situ*
719 chloroform measurements at AGAGE atmospheric research stations from 1994 –1998, J.
720 Geophys. Res., 106, No. D17, 20,429-20,444, ISSN: 0747-7309, 2001.

721 O’Doherty, S., Cunnold, D. M., Miller, B. R., Mühle, J., McCulloch, A., Simmonds, P. G.,
722 Manning, A. J., Reimann, S., Vollmer, M. K., Grealley, B. R., Prinn, R. G., Fraser, P. J., Steele,
723 P., Krummel, P. B., Dunse, B. L., Porter, L. W., Lunder, C. R., Schmidbauer, N., Hermansen,
724 O., Salameh, P. K., Harth, C. M., Wang, R. H. J., and Weiss, R. F.: Global and regional
725 emissions of HFC-125 (CHF₂CF₃) from *in situ* and air archive atmospheric observations at
726 AGAGE and SOGE Observatories, J. Geophys. Res., 114, D23304, 2009.

727 Oram, D.E., Sturges, W. T., Penkett, S. A., McCulloch, A., and Fraser, P. J.: Growth of
728 fluoroform (CHF₃, HFC-23) in the background atmosphere, Geophys. Res. Lett., 25, 35-38,
729 1998.

730 Prinn, R. G., Weiss, R. F., Fraser, P. J., Simmonds, P. G., Cunnold, D. M., Alyea, F. N.,
731 O’Doherty, S., Salameh, P. K., Miller, B. R., Huang, J., Wang, R. H. J., Hartley, D. E., Harth,
732 C., Steele, L. P., Sturrock, G., Midgley, P. M., and McCulloch, A.: A history of chemically and
733 radiatively important gases in air deduced from ALE/GAGE/AGAGE, J. Geophys. Res., 105
734 (D14), 17751-17792, doi: 10.1029/2000JD900141, 2000.

735 Rigby, M., Ganesan, A.L., and Prinn, R.G.: Deriving emissions time series from sparse
736 atmospheric mole fractions, J. Geophys. Res., 116, D08306, doi:10.1029/2010JD015401, 2011.

737 Rigby, M., Prinn, R. G., O’Doherty, S., Montzka, S. A., McCulloch, A., Harth, C. M., Mühle, J.,
738 Salameh, P. K., Weiss, R. F., Young., D., Simmonds, P. G.: Hall, B. D., Dutton, G. S., Nance,
739 D., Mondeel, D. J., Elkins, J. W., Krummel, P. B., Steele, L. P., and Fraser, P. J.: Re-evaluation
740 of the lifetimes of the major CFCs and CH₃Cl₃ using atmospheric trends, Atmos. Chem. Phys.,
741 13, 1-11, doi:10.5194/acp-13-1-2013, 2013.

742 Rigby, M., Prinn, R. G., O’Doherty, S., Miller, B. R., Ivy, D., Mühle, J., Harth, C. M., Salameh,
743 P. K., Arnold, T., Weiss, R. F., Krummel, P. B., Steele, P. L., Fraser, P. J., Young., D., and
744 Simmonds, P. G.: Recent and future trends in synthetic greenhouse gas radiative forcing,
745 Geophys. Res. Lett., 41, 2623–2630, 2014.

746 Rigby, M., Montzka, S. A., Prinn, R. G., White, J. W. C., Young, D., O'Doherty, S., Lunt, M. F.,
747 Ganesan, A. L., Manning, A. J., Simmonds, P. G., Salameh, P. K., Harth, C. M., Mühle, J.,
748 Weiss, R. F., Fraser, P. J., Steele, L. P., Krummel, P. B., McCulloch, A. and Park, S.: Role of
749 atmospheric oxidation in recent methane growth, *Proceedings of the National Academy of*
750 *Sciences*, 201616426, doi:[10.1073/pnas.1616426114](https://doi.org/10.1073/pnas.1616426114), 2017

751 Ruckstuhl, A. F., Henne, S., Reimann, S., Steinbacher, M., Vollmer, M. K., O'Doherty, S.,
752 Buchmann, B., and Hueglin, C.: Robust extraction of baseline signal of atmospheric trace
753 species using local regression, *Atmos. Meas. Tech.*, 5, 2613-2624, doi: 10.5194/amt-5-2613-
754 2012, 2012.

755 Schönenberger, F., Henne, S., Hill, M., Vollmer, M.K., Kouvarakis, G., Mihalopoulos, N.,
756 O'Doherty, S., Maione, M., Emmenegger, L., Peter, T., and Reimann, S. Abundance and sources
757 of atmospheric halocarbons in the eastern Mediterranean, *Atmos. Chem. Phys. Discuss.* 2017.
758 doi.org/10.5194/acp-2017-451.

759 Simmonds, P. G., M. Rigby, M., McCulloch, A., O'Doherty, S., Young, D., Mühle, J.,
760 Krummel, P.B., Steele, L.P., Fraser, P.J., Manning, A.J., Weiss, R. F., Salameh, P. K., Harth, C.
761 M., Wang, R. H. J., and Prinn, R.G.: Changing trends and emissions of
762 hydrochlorofluorocarbons (HCFCs) and their hydrofluorocarbons (HFCs) replacements, *Atmos.*
763 *Chem. Phys.* 17, 4641-4655, doi:10.5194/acp-17-4641-2017.

764 SPARC Report on the Lifetimes of Stratospheric Ozone-Depleting Substances, Their
765 Replacements, and Related Species, edited by Ko, M., Newman, P., Reimann, S., and Strahan, S,
766 SPARC Report No. 6, WCRP-15/2013, 2013.

767 Spivakovsky, C. M., Logan, J. A., Montzka, S. A., Balkanski, Y. J., Foreman-Fowler, M., Jones,
768 D. B. A., Horowitz, L. W., Fusco, A. C., Brenninkmeijer, C. A. M., Prather, M. J., Wofsy, S. C.,
769 and McElroy, M. B.: Three-dimensional climatological distribution of tropospheric OH: Update
770 and evaluation, *J. Geophys. Res.*, 105, 8931–8980, 2000.

771 Stohl, A., Forster, C., Frank, A., Seibert, P., and Wotawa, G.: Technical note: The Lagrangian
772 particle dispersion model FLEXPART version 6.2, *Atmos. Chem. Phys.*, 5, 2461-2474, doi:
773 10.5194/acp-5-2461-2005, 2005.

774 Stohl, A.; Kim, J.; Li, S.; O'Doherty, S.; Mühle, J.; Salameh, P. K.; Saito, T.; Vollmer, M. K.;
775 Wan, D.; Weiss, R. F.; Yao, B.; Yokouchi, Y.; Zhou, L. X.: Hydrochlorofluorocarbon and
776 hydrofluorocarbon emissions in East Asia determined by inverse modelling, *Atmos. Chem.*
777 *Phys.* 10, 3545–3560, 2010.

778 TEAP (Technology and Economic Assessment Panel of the Montreal Protocol), 2006
779 Assessment Report, United Nations Environment Programme, Nairobi, Kenya, 2006.

780 Trudinger, C. M., Enting, I. G., Etheridge, D. M., Francey, R. J., Levchenko, V. A., Steele, L. P.,
781 Raynaud, D., and Arnaud, L.: Modelling air movement and bubble trapping in firn, *J. Geophys.*
782 *Res.*, 102, 6747–6763, doi:10.1029/96JD03382, 1997.

783 Trudinger, C. M., Etheridge, D. M., Rayner, P. J., Enting, I. G., Sturrock, G. A., and
784 Langenfelds, R. L.: Reconstructing atmospheric histories from measurements of air composition
785 in firn, *J. Geophys. Res.*, 107, 4780, doi:10.1029/2002JD002545, 2002.

786 Trudinger, C. M., Enting, I. G., Rayner, P. J., Etheridge, D. M., Buizert, C., Rubino, M.,
787 Krummel, P. B., and Blunier, T.: How well do different tracers constrain the firn diffusivity
788 profile? *Atmos. Chem. Phys.*, 13, doi:10.5194/acp-13-1485-2013, 2013.

789 Trudinger, C. M., Fraser, P. J., Etheridge, D. M., Sturges, W. T., Vollmer, M. K., Rigby, M.,
790 Martinierie, P., Mühle, J. Worton, D. R., Krummel, P. B., Steele, L. P., Miller, B. R., Laube,
791 J., Mani, F., Rayner, P. J., Harth, C. M., Witrant, E., Blunier, T., Schwander, J., O'Doherty, S.,
792 and Battle, M.: Atmospheric abundance and global emissions of perfluorocarbons CF₄, C₂F₆ and
793 C₃F₈ since 1800 inferred from ice core, firn, air archive and *in situ* measurements, *Atmos. Chem.*
794 *Phys.*, 16, 11 733–11 754, doi:10.5194/acp-16-11733-2016, 2016.

795 UNEP (2009). (United Nations Environment Programme), HCFC Production Data,
796 http://ozone.unep.org/Data_Access/, U.N. Environ. Programme. Nairobi, 2009.

797 UNEP (2017a). Key aspects related to HFC-23 by-product control technologies
798 UNEP./OzL.Pro/ExCom/78/9. 7 March 2017.

799 UNEP (2017b). Production and Consumption of Ozone Depleting Substances under the
800 Montreal Protocol, 1986-2015, United Nations Environment Programme, available at
801 <http://ozone.unep.org/en/data-reporting/data-centre>

802 UNFCCC (2009). (United Nations Framework Convention on Climate Change), Greenhouse
803 Gas Emissions Data, available at http://unfccc.int/ghg_data/ghg_data_unfccc/items/4146.php,
804 U.N. Framework Conv. on Climate Change, Bonn, Germany, 2009.

805 UNFCCC (2017), Greenhouse Gas Emissions Data, U.N. Framework Conv, on Clim. Change,
806 Bonn, Germany, available at
807 [http://unfccc.int/national_reports/annex_i_ghg_inventories/national_inventories_submissions/it](http://unfccc.int/national_reports/annex_i_ghg_inventories/national_inventories_submissions/items/10116.php)
808 [ems/10116.php](http://unfccc.int/national_reports/annex_i_ghg_inventories/national_inventories_submissions/items/10116.php)

809 USEPA, (2013). Global mitigation of non-CO₂ greenhouse gases: 2010-2030, United States
810 Environmental Protection Agency, EPA-430-R-13-011, September 2013.

811 Vollmer, M. K., Mühle, J., Trudinger, C. M., Rigby, M., Montzka, S. A., Harth, C. M., Miller,
812 B. R., Henne, S., Krummel, P. B., Hall, B. D., Young, D., Kim, J., Arduini, J., Wenger, A., Yao,
813 B., Reimann, S., O'Doherty, S., Maione, M., Etheridge, D. M., Li, S., Verdonik, D. P., Park, S.,
814 Dutton, G., Steele, L. P., Lunder, C. R., Rhee, T. S., Hermansen, O., Schmidbauer, N., Wang, R.
815 H. J., Hill, M., Salameh, P. K., Langenfelds, R. L., Zhou, L., Blunier, T., Schwander, J., Elkins,
816 J. W., Butler, J. H., Simmonds, P. G., Weiss, R. F., Prinn, R. G., and Fraser, P. J.: Atmospheric
817 histories and global emissions of halons H-1211 (CBrClF₂), H-1301 (CBrF₃), and H-2402
818 (CBrF₂CBrF₂), *J. Geophys. Res. Atmos.*, 121, 3663–3686, doi:10.1002/2015JD024488, 2016.

819 Vollmer, M. K., Young, D., Trudinger, C.M., Mühle, J., Henne, S., Rigby, M., Park, S., Li, S.,
820 Guillevic, M., Mitrevski, B., Harth, C. M., Miller, B. R., Reimann, S., Yao, B., Steele, L. P.,
821 Wyss, S.A., Lunder, C.R., Arduini, J., McCulloch, A., Wu, S., Rhee, T.S., Wang, R. H. J.,
822 Salameh, P. K., Hermansen, O., Hill, M., Langenfelds, R. L., Ivy, D., O'Doherty, S., Krummel,
823 P. B., Maione, M., Etheridge, D. M., Zhou, L., Fraser, P. J., Prinn, R. G., Weiss, R. F.
824 Simmonds, P. G: Atmospheric histories and emissions of chlorofluorocarbons CFC-13 (CClF₃),
825 ΣCFC-114 (C₂Cl₂F₄), and CFC-115 (C₂ClF₅), *Atmos.Chem. Phys.*,18, 979-1002, 2018.

826 Yao, B., Vollmer, M. K., Zhou, L. X., Henne, S., Reimann, S., Li, P. C., Wenger, A., and Hill,
827 M. 2012.: In-situ measurements of atmospheric hydrofluorocarbons (HFCs) and
828 perfluorocarbons (PFCs) at the Shangdianzi regional background station, China, Atmos. Chem.
829 Phys, 12, 10181-10193; doi:10.5194/acp-12-10181-2012.

830 Yokouchi, Y; Taguchi, S., Saito, T., Tohjima, Y., Tanimoto, H., and Mukai, H.: High frequency
831 measurements of HFCs at a remote site in East Asia and their implications for Chinese
832 emissions, Geophys. Res. Lett, 33, doi:10.1029/2006GL026403, 2006.

833 Xiang, B., Prabir, P. K., Montzka, S. A., Miller, S. M., W. Elkins, J. W., Moore, F. L., Atlas, E.
834 L., Miller, B. R., Weiss, R. F., Prinn, R. G. and Wofsy, S. C.: Global emissions of refrigerants
835 HCFC-22 and HFC-134a: Unforeseen seasonal contributions, PNAS 2014
836 December, 111 (49) 17379-17384. (<https://doi.org/10.1073/pnas.1417372111>).

837
838 **Data availability**

839
840 The entire ALE/GAGE/AGAGE data base comprising every calibrated measurement including pollution
841 events is archived with the Carbon Dioxide Information and Analysis Center (CDIAC) at the U.S.
842 Department of Energy, Oak Ridge National Laboratory (<http://cdiac.ornl.gov> and also
843 (<http://agage.mit.edu/data/agage-data>).

844
845 Table 1. AGAGE sites used in this study, their coordinates and start dates for GC-MS-Medusa
846 measurements of HFC-23 and HCFC-22.

847

AGAGE Site	Latitude	Longitude	HFC-23	HCFC-22
Mace Head (MHD), Ireland ¹	53.3° N	9.9° W	Oct. 2007	Nov. 2003
Trinidad Head (THD), California, USA	41.0° N	124.1° W	Sep. 2007	Mar. 2005
Ragged Point (RPB), Barbados	13.2° N	59.4° W	Aug. 2007	May. 2005
Cape Matatula (SMO), American Samoa	14.2° S	170.6° W	Oct. 2007	May. 2006
Cape Grim (CGO), Tasmania, Australia	40.7° S	144.7° E	Nov. 2007	Jan 2004
Jungfrauoch, Switzerland ¹	46.5°N	8.0°E	Apr. 2008	Aug. 2012
Cape Grim Air Archive			Apr. 1978	Apr. 1978

848

849 ¹ Observations used for regional European emissions

850

851

852

853 Table 2. Annual mean global HFC-23 emissions, mole fractions, and growth rates, derived from
 854 the AGAGE 12-box model.

Year	HFC-23 global annual emissions (Gg yr ⁻¹) ±1 sigma (σ) SD.	HFC-23 global mean mole fraction (pmol mol ⁻¹) ±1 sigma (σ) SD.	HFC-23 global growth rate (pmol mol ⁻¹ yr ⁻¹) ±1 sigma (σ) SD.
1980	4.2 ± 0.7	3.9 ± 0.1	0.33 ± 0.05
1981	4.2 ± 0.8	4.3 ± 0.1	0.33 ± 0.05
1982	4.4 ± 0.7	4.6 ± 0.1	0.35 ± 0.07
1983	5.2 ± 0.7	5.0 ± 0.1	0.41 ± 0.05
1984	5.6 ± 0.7	5.4 ± 0.1	0.44 ± 0.05
1985	5.8 ± 0.8	5.9 ± 0.1	0.45 ± 0.05
1986	5.8 ± 0.7	6.3 ± 0.1	0.45 ± 0.05
1987	5.9 ± 0.7	6.8 ± 0.1	0.46 ± 0.05
1988	6.8 ± 0.7	7.2 ± 0.1	0.52 ± 0.05
1989	7.1 ± 0.7	7.8 ± 0.2	0.55 ± 0.05
1990	7.0 ± 0.7	8.3 ± 0.2	0.54 ± 0.05
1991	7.0 ± 0.7	8.9 ± 0.2	0.54 ± 0.05
1992	7.4 ± 0.6	9.4 ± 0.2	0.57 ± 0.05
1993	7.9 ± 0.6	10.0 ± 0.2	0.61 ± 0.04
1994	8.3 ± 0.7	10.6 ± 0.2	0.64 ± 0.04
1995	8.9 ± 0.6	11.3 ± 0.2	0.69 ± 0.05
1996	9.6 ± 0.6	12.0 ± 0.2	0.74 ± 0.04
1997	10.1 ± 0.6	12.8 ± 0.3	0.77 ± 0.04
1998	10.4 ± 0.7	13.6 ± 0.3	0.79 ± 0.04
1999	10.9 ± 0.7	14.4 ± 0.3	0.82 ± 0.04
2000	10.4 ± 0.8	15.2 ± 0.3	0.76 ± 0.05
2001	9.4 ± 0.7	15.9 ± 0.3	0.68 ± 0.05
2002	9.5 ± 0.7	16.6 ± 0.3	0.69 ± 0.05
2003	10.3 ± 0.8	17.3 ± 0.3	0.77 ± 0.05
2004	11.8 ± 0.8	18.1 ± 0.3	0.90 ± 0.05
2005	13.2 ± 0.8	19.1 ± 0.4	1.01 ± 0.05
2006	13.3 ± 0.8	20.1 ± 0.4	0.99 ± 0.05
2007	11.7 ± 0.7	21.0 ± 0.4	0.85 ± 0.04
2008	11.2 ± 0.6	21.9 ± 0.4	0.78 ± 0.03
2009	9.6 ± 0.6	22.6 ± 0.4	0.68 ± 0.03
2010	10.4 ± 0.6	23.3 ± 0.4	0.74 ± 0.03
2011	11.6 ± 0.6	24.1 ± 0.5	0.85 ± 0.03
2012	12.9 ± 0.6	25.0 ± 0.5	0.96 ± 0.03
2013	14.0 ± 0.6	26.0 ± 0.5	1.04 ± 0.03
2014	14.5 ± 0.6	27.0 ± 0.5	1.05 ± 0.03
2015	13.1 ± 0.7	28.0 ± 0.5	0.95 ± 0.03
2016	12.7 ± 0.6	28.9 ± 0.6	0.94 ± 0.03

855 Note: Data are tabulated as annual mean mid-year values.

856 Earlier emissions estimates (1930-1979) determined from the AGAGE 12-box model are
 857 listed in Supplementary Material (6), Table S5.

858

859 Table 3. Annual mean global HCFC-22 emissions, mole fractions, and growth rates, derived
 860 from the AGAGE 12-box model.

Year	HCFC-22 global annual emissions (Gg yr ⁻¹) ±1 sigma (σ) SD.	HCFC-22 global mean mole fraction (pmol mol ⁻¹) ±1 sigma (σ) SD.	HCFC-22 global growth rate (pmol mol ⁻¹ yr ⁻¹) ±1 sigma (σ) SD.
1980	116.8 ± 17.6	41.6 ± 1.0	4.1 ± 0.9
1981	123.4 ± 18.8	45.8 ± 1.2	4.2 ± 0.8
1982	125.7 ± 15.7	49.9 ± 1.3	4.0 ± 0.8
1983	125.2 ± 20.1	53.7 ± 0.9	3.6 ± 1.0
1984	136.8 ± 18.1	57.3 ± 1.1	4.2 ± 0.6
1985	166.1 ± 17.0	62.2 ± 1.0	5.7 ± 0.7
1986	174.2 ± 19.3	68.5 ± 1.0	5.5 ± 0.7
1987	155.4 ± 20.2	72.9 ± 1.2	4.1 ± 0.7
1988	177.8 ± 19.6	77.2 ± 1.0	5.0 ± 0.7
1989	198.0 ± 19.8	82.9 ± 1.0	6.0 ± 0.7
1990	209.1 ± 19.7	89.1 ± 1.2	6.2 ± 0.6
1991	212.2 ± 21.4	95.1 ± 1.2	5.8 ± 0.7
1992	207.1 ± 23.9	100.5 ± 1.3	5.0 ± 0.6
1993	214.6 ± 22.8	105.4 ± 1.3	5.0 ± 0.6
1994	222.7 ± 22.9	110.4 ± 1.3	5.2 ± 0.5
1995	241.4 ± 26.9	115.9 ± 1.3	5.7 ± 0.5
1996	230.1 ± 24.3	121.4 ± 1.3	4.8 ± 0.5
1997	238.3 ± 24.1	125.8 ± 1.3	5.0 ± 0.5
1998	256.0 ± 27.2	131.7 ± 1.3	5.7 ± 0.4
1999	251.8 ± 28.4	136.8 ± 1.4	5.0 ± 0.3
2000	275.1 ± 28.7	142.0 ± 1.4	5.8 ± 0.2
2001	275.3 ± 28.8	147.9 ± 1.5	5.5 ± 0.2
2002	280.7 ± 31.6	153.1 ± 1.6	5.3 ± 0.2
2003	286.3 ± 30.1	158.3 ± 1.6	5.3 ± 0.2
2004	292.1 ± 30.6	163.7 ± 1.7	5.3 ± 0.2
2005	312.3 ± 34.6	169.2 ± 1.6	6.1 ± 0.2
2006	334.3 ± 35.0	175.9 ± 1.7	7.2 ± 0.2
2007	355.6 ± 35.2	183.6 ± 1.8	8.0 ± 0.2
2008	372.9 ± 38.4	191.9 ± 1.9	7.9 ± 0.2
2009	368.6 ± 39.7	199.2 ± 2.0	7.4 ± 0.2
2010	385.8 ± 41.3	206.8 ± 2.0	7.4 ± 0.3
2011	373.1 ± 41.3	213.7 ± 2.1	6.2 ± 0.2
2012	373.2 ± 45.5	219.3 ± 2.2	5.5 ± 0.2
2013	369.6 ± 44.1	224.7 ± 2.3	5.0 ± 0.2
2014	373.9 ± 45.7	229.5 ± 2.3	4.6 ± 0.2
2015	364.2 ± 47.7	233.7 ± 2.2	3.9 ± 0.2
2016	370.3 ± 45.9	237.5 ± 2.2	3.9 ± 0.2

861 Note: Data are tabulated as annual mean mid-year values. These HCFC-22 global emissions
 862 estimates are updates of the HCFC-22 emissions reported in Simmonds et al. (2017) for the
 863 period 1995-2015.

864
 865

866

867 Table 4: European HFC-23 emissions (tonne, Mg) by country/region: E_a *a priori*, E_b *a posteriori*
 868 emissions, f_a fraction of *a priori* emissions from factory locations, f_b fraction of *a posteriori*
 869 emissions from factory locations. All values represent averages from both inversions using
 870 different *a priori* distributions.

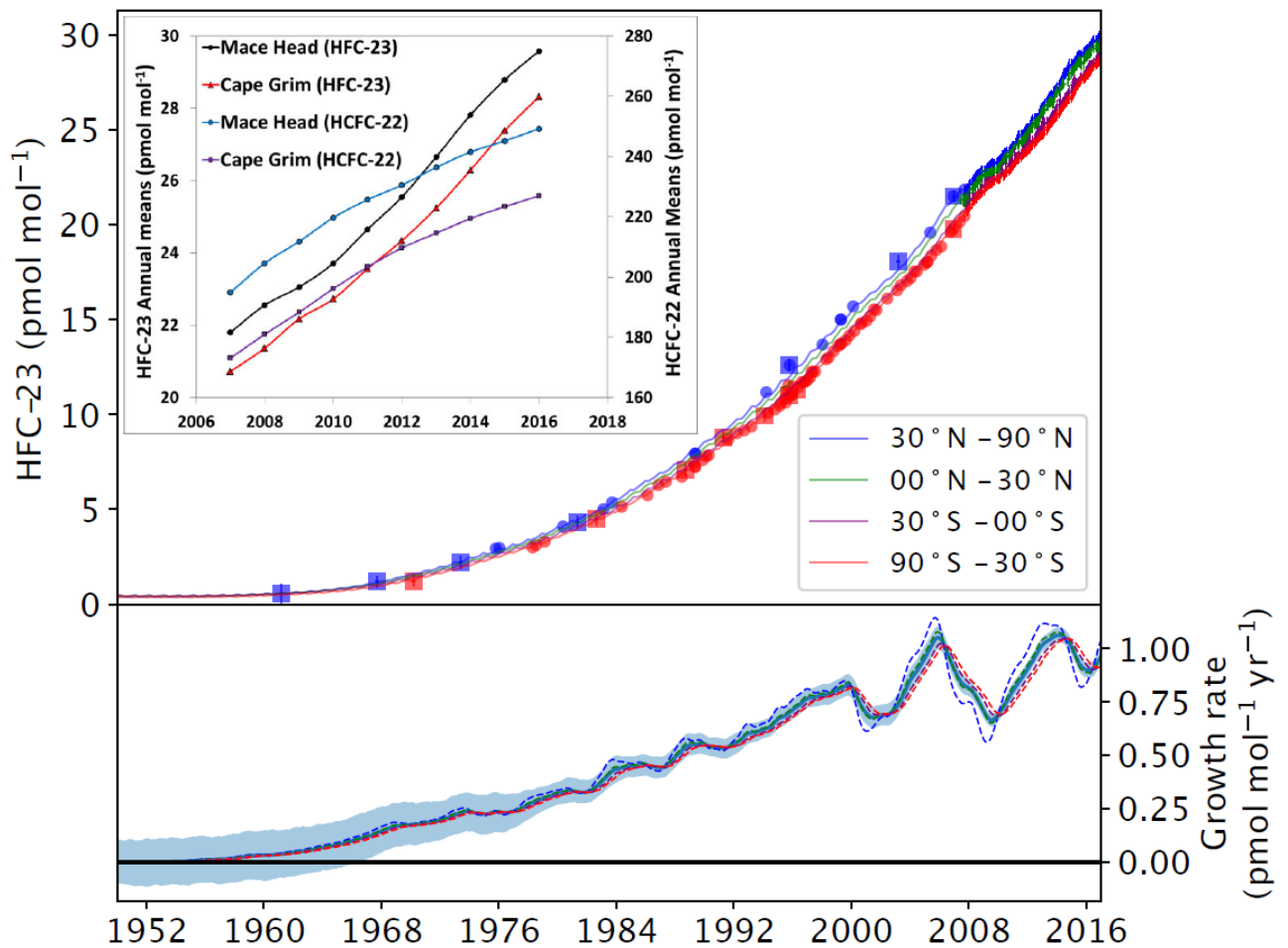
871

year	Germany				France				Italy			
	E_a (Mg/yr)	E_b (Mg/yr)	f_a (%)	f_b (%)	E_a (Mg/yr)	E_b (Mg/yr)	f_a (%)	f_b (%)	E_a (Mg/yr)	E_b (Mg/yr)	f_a (%)	f_b (%)
2009	8±16	34±12	30	49	15±31	2±3.2	88	6	8.4±17	34±8.7	26	52
2010	7.6±15	19±14	27	13	12±23	15±5.1	84	86	9±18	48±9.3	26	45
2011	8±16	44±13	33	58	7.7±15	10±3.4	70	73	9.2±18	34±11	26	43
2012	7.6±15	32±9.7	30	40	8.1±16	8.3±3.4	76	73	9.1±18	25±8.6	26	31
2013	7.2±14	16±9.4	28	58	9.2±18	27±16	82	93	9.3±19	47±24	26	29
2014	7.1±14	20±9.2	30	27	9.4±19	10±2.3	84	85	9.5±19	32±14	26	32
2015	6.6±13	12±8.7	29	14	9.5±19	17±3.9	86	92	9.8±20	37±19	26	24
2016	6.6±13	19±9.1	29	26	9.5±19	9.9±3.4	86	85	9.8±20	23±10	26	39

year	Benelux				United Kingdom				Iberian Peninsula			
	E_a (Mg/yr)	E_b (Mg/yr)	f_a (%)	f_b (%)	E_a (Mg/yr)	E_b (Mg/yr)	f_a (%)	f_b (%)	E_a (Mg/yr)	E_b (Mg/yr)	f_a (%)	f_b (%)
2009	13±27	25±8.8	98	99	3.8±7.6	5.3±3.1	84	87	97±190	56±29	57	10
2010	34±67	16±7.1	99	98	1.2±2.3	2.8±1.9	48	71	130±260	120±33	66	52
2011	15±29	21±16	97	97	1±2.1	1.5±1.7	39	21	83±170	75±27	50	27
2012	11±22	53±13	96	99	0.92±1.8	2±1.6	26	46	74±150	46±27	45	43
2013	16±33	94±13	98	100	1.1±2.1	2.1±1.8	29	48	64±130	110±27	38	22
2014	3.8±7.6	11±6.3	85	94	1.3±2.5	6.8±2.4	35	73	59±120	55±27	35	45
2015	8.7±17	20±12	94	97	1.4±2.7	2.5±2.1	34	37	48±96	19±18	26	9
2016	8.7±17	45±11	94	99	1.4±2.7	3.8±2.2	34	42	48±96	69±24	26	33

872 Note : **Benelux** (Belgium, the Netherlands, and Luxembourg).

873



874

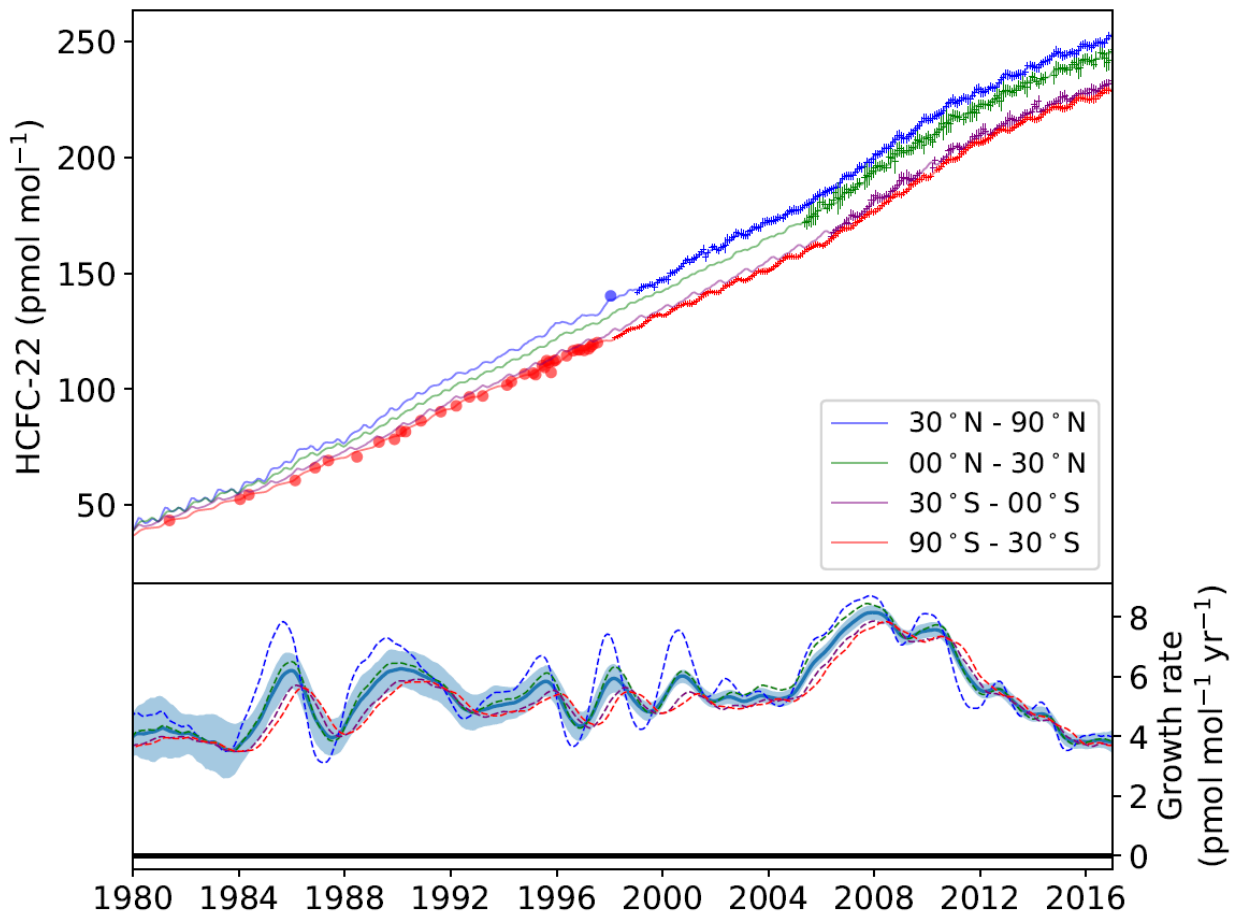
875 Figure 1. HFC-23 modelled mole fractions for the four equal-mass latitudinal subdivisions of the
 876 global atmosphere calculated from the 12-box model and the *in situ* records from the AGAGE
 877 core sites (points with error bars), firm air (squares, red SH, blue NH), old NH air data (blue
 878 circles, only shown for times without NH *in situ* data), and CGAA data (red circles, only shown
 879 for times without SH *in situ* data). Lower box shows the annual growth rates (global – blue solid
 880 line with uncertainty band - and individual semi-hemispheres – dashed lines) in $\text{pmol mol}^{-1} \text{ yr}^{-1}$.
 881 Figure 1 inset, compares the annual mean mole fractions of HFC-23 and HCFC-22 recorded at
 882 Mace Head and Cape Grim from 2007-2016.

883

884

885

886



887

888 Figure 2. HCFC-22 modelled mole fractions for the four equal-mass latitudinal subdivisions of
 889 the global atmosphere calculated from the 12-box model and the *in situ* records from the
 890 AGAGE core sites (points with error bars) and CGAA data (red circles, only shown for times
 891 without *in situ* data) and old NH air data (blue circles, only shown for times without NH *in situ*
 892 data). Lower box shows the annual growth rates (global – blue solid line with uncertainty band -
 893 and individual semi-hemispheres – dashed lines) in $\text{pmol mol}^{-1} \text{ yr}^{-1}$.

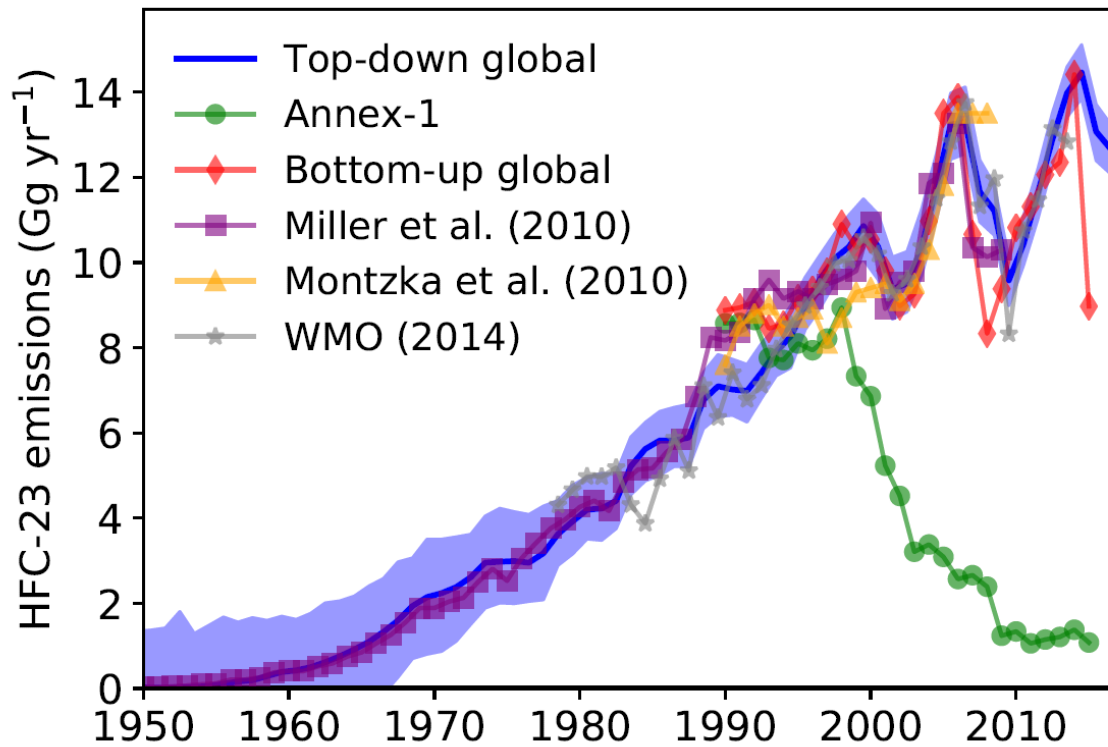
894

895

896

897

898



899

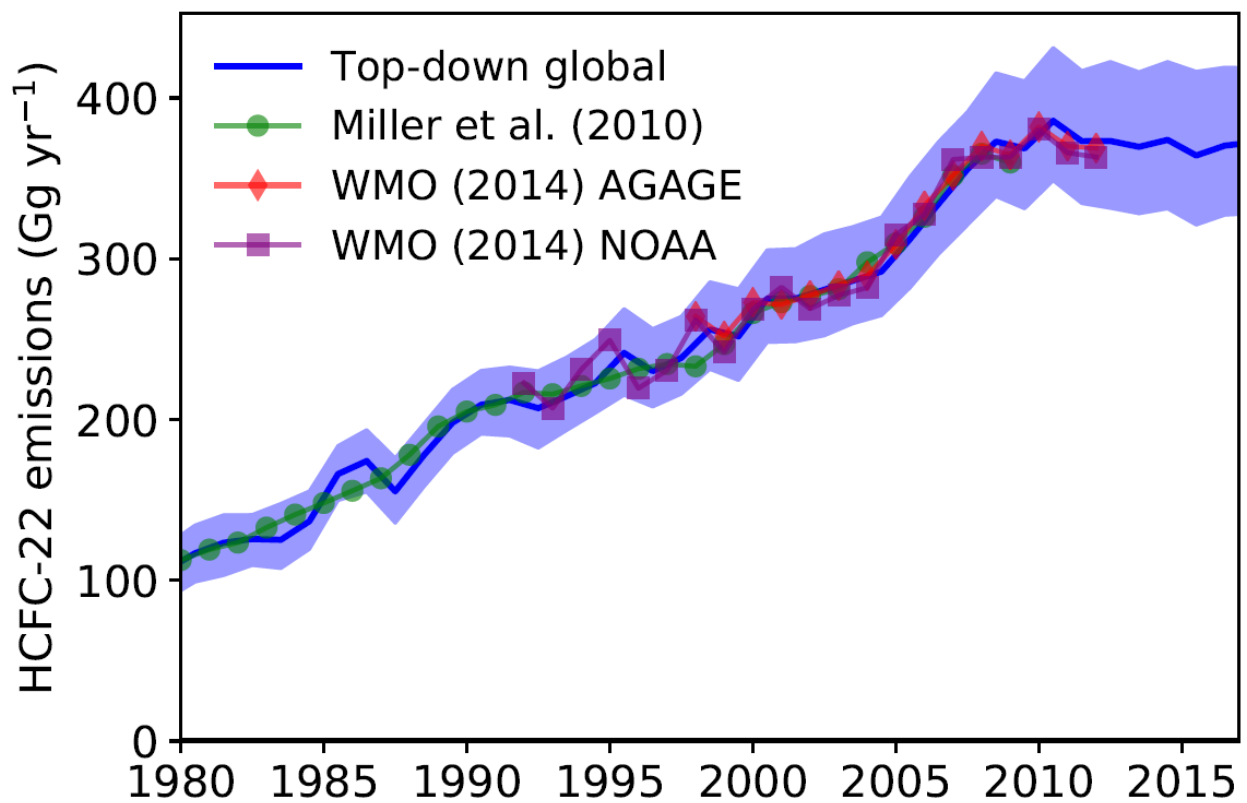
900 Figure 3. Global emissions of HFC-23 calculated from the AGAGE 12-box model (blue line and
 901 shading, 1σ uncertainty). Data are plotted as annual mean values, centred on the middle of each
 902 year. The purple line shows bottom-up HFC-23 estimates of emissions from Miller et al. (2010),
 903 the yellow line HFC-23 emissions estimates from Montzka et al. (2010) and the grey line from
 904 Carpenter and Reimann (WMO 2014). The green line shows emissions reports by Annex-1
 905 countries. The red line shows the bottom-up estimated global emissions developed here and
 906 discussed in (Supplementary Material 3).

907

908

909

910



912

913 Figure 4. Global emissions of HCFC-22 calculated from the AGAGE 12-box model (blue line
 914 and shading, 1σ uncertainty). Data are plotted as annual mean mid-year values. The green line
 915 shows bottom-up HCFC-22 estimates of emissions from Miller et al. (2010). Red and purple
 916 lines show HCFC-22 emissions calculated from AGAGE and NOAA data/models respectively,
 917 reported in WMO 2014 (Carpenter and Reimann, 2014).

918

919

920

921

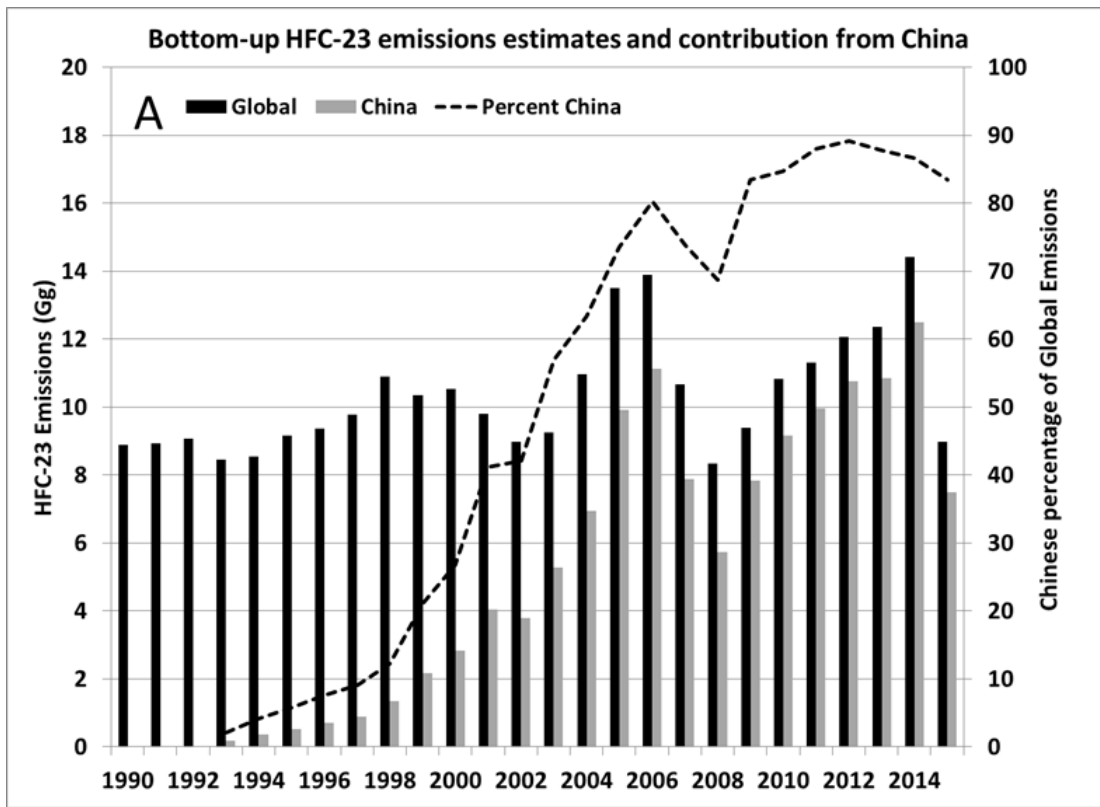
922

923

924

925

926
927
928
929
930
931
932
933
934
935
936
937
938
939
940
941
942
943
944
945
946
947
948
949
950
951
952



F

Figure 5a. HFC-23 global and Chinese emissions estimates and the percentage of Chinese emissions contributing to the global total (dashed line). Compiled from Table S4 in Supplementary Material (3).

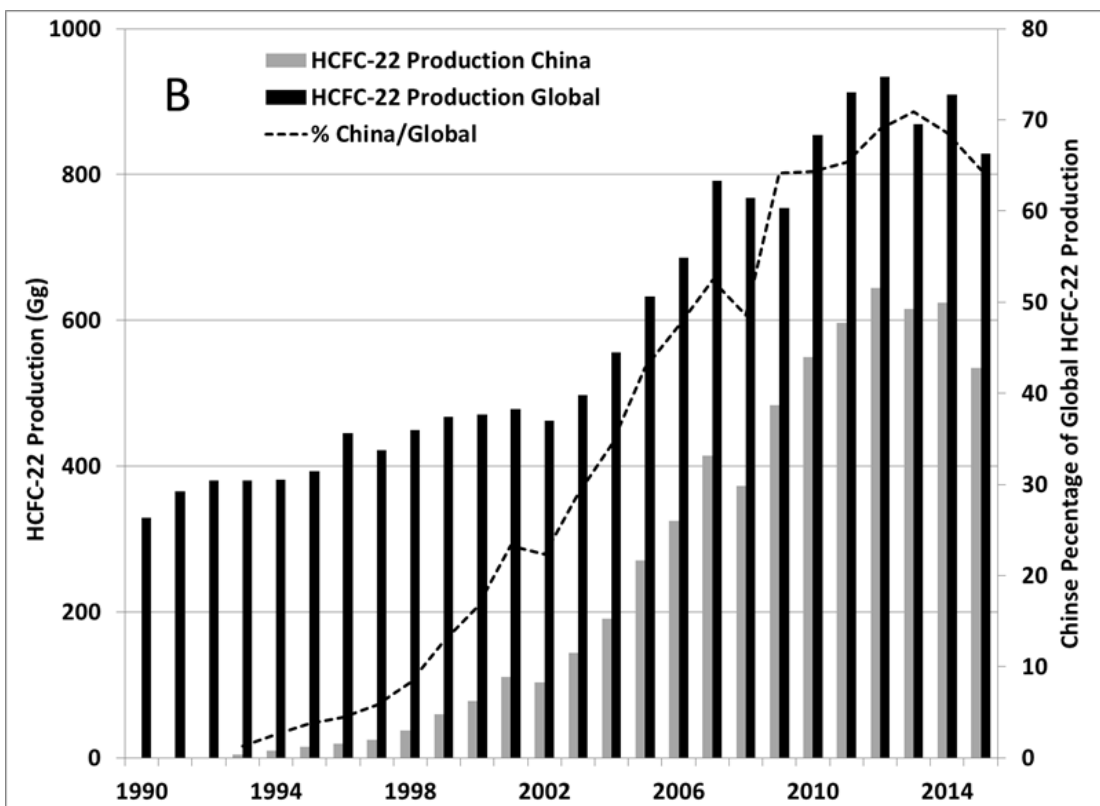


Figure 5b. HCFC-22 emissions estimates of global and Chinese production and the percentage of Chinese production as a fraction of the global total (dashed line). Compiled from Table S3 in Supplementary Material (3).

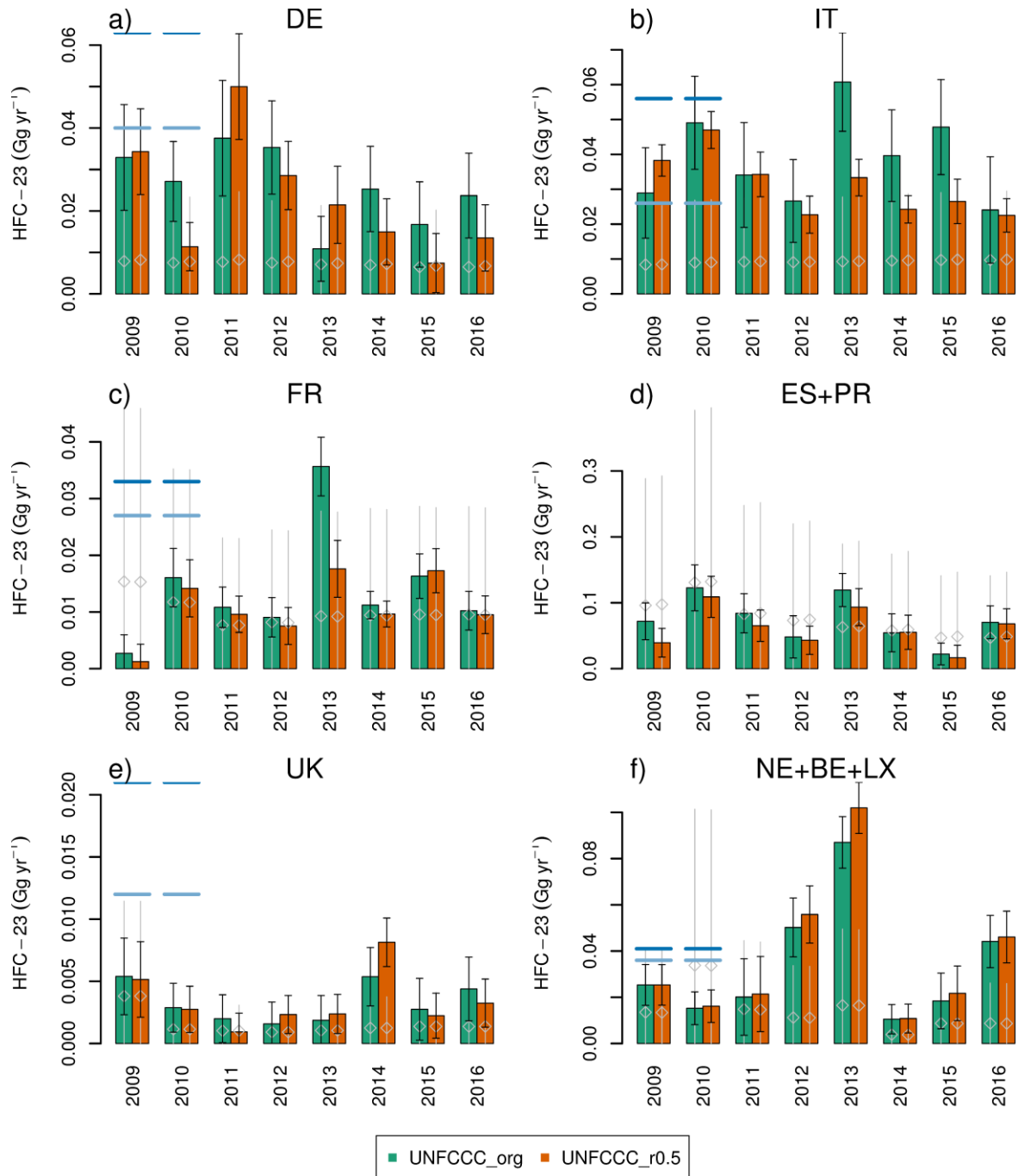


Figure 6: Temporal evolution of national/regional emissions of HFC-23: solid bars and error bars give *a posteriori* emissions using the two sets of *a priori* emissions (grey lines). The two approaches (green and orange bars) spatially distribute these different bottom-up estimates (see section 2.7.3). Blue horizontal lines give the estimates of Keller et al. (2011) for their Bayesian (light blue) and point source (dark blue) estimate; a) Germany (DE), b) Italy (IT), c) France (FR), d) Spain and Portugal (ES+PR), e) United Kingdom (UK), f) Benelux countries (Netherlands, Belgium, Luxembourg, NE+BE+LX).

Supplementary Material

Recent increases in the growth rate and emissions of HFC-23 (CHF₃) and the link to HCFC-22 (CHClF₂) production

Peter G. Simmonds¹, Matthew Rigby¹, Archie McCulloch¹, Martin K. Vollmer², Stephan Henne², Jens Mühle³, Simon O'Doherty¹, Alistair J. Manning⁴, Paul B. Krummel⁵, Paul J. Fraser⁵, Dickon Young¹, Ray F. Weiss³, Peter K. Salameh³, Christina M. Harth³, Stefan Reimann², Cathy M. Trudinger⁵, L. Paul Steele⁵, Ray H. J. Wang⁶, Diane J. Ivy⁷, Ronald G. Prinn⁷, Blagoj Mitrevski⁵, and David M. Etheridge⁵.

¹ Atmospheric Chemistry Research Group, University of Bristol, Bristol, UK

² Swiss Federal Laboratories for Materials Science and Technology, Laboratory for Air Pollution and Environmental Technology (Empa), Dübendorf, Switzerland,

³ Scripps Institution of Oceanography (SIO), University of California at San Diego, La Jolla, California, USA

⁴ Met Office Hadley Centre, Exeter, UK

⁵ Climate Science Centre, Commonwealth Scientific and Industrial Research Organisation (CSIRO) Oceans and Atmosphere, Aspendale, Victoria, Australia

⁶ School of Earth, and Atmospheric Sciences, Georgia Institute of Technology, Atlanta, Georgia, USA

⁷ Center for Global Change Science, Massachusetts Institute of Technology, Cambridge, Massachusetts, USA

Correspondence to: P.G. Simmonds (petersg@aol.com)

Supplementary Material (1): AGAGE Instrumentation and Measurement Techniques

Typically for each measurement, the analytes from two litres of air are collected on the microtrap and, after fractionated distillation, purification and transfer, are desorbed onto a single main capillary chromatography column (CP-PoraBOND Q, 0.32 mm ID × 25 m, 5 µm, Agilent Varian Chrompack, batch-made for AGAGE applications) purged with helium (research grade 6.0) that is further purified using a heated helium purifier (HP2, VICI, USA). Separation and detection of the compounds are achieved by using Agilent Technology GCs (model 6890N) and quadrupole mass spectrometers in selected ion mode (initially model 5973 series, progressively converted to 5975C over the later years).

The quaternary standards are whole-air samples, pressurized into 34 L internally electropolished stainless steel canisters (Essex Industries, USA). They are filled by the responsible station scientist and/or on-site station personnel who are in charge of the respective AGAGE remote sites using modified oil-free diving compressors (SA-3 and SA-6, RIX Industries, USA) to ~60 bar (older canisters to ~40 bar). Cape Grim is an exception, where the canisters used for quaternary standard purposes are filled cryogenically. This method of cryogenically collecting large volumes of ambient air is the same as that is used for collecting air for the CGAA and measurements of many atmospheric trace species in air samples collected in

this manner show that the trace gas composition of the air is well preserved (Fraser et al., 1991, 2016; Langenfelds et al., 1996, 2003). The on-site quaternary standards are compared weekly to tertiary standards from the central calibration facility at the Scripps Institution of Oceanography (SIO) in order to propagate the primary calibration scales and assess any long-term drifts. These tertiary standards are filled with ambient air in Essex canisters under “baseline” clean air conditions at Trinidad Head or at La Jolla (California) and are measured at SIO against secondary ambient air standards (to obtain an “out” value) before they are shipped to individual AGAGE sites. We define “baseline” as air masses that are representative of the unpolluted marine boundary layer, uninfluenced by recent local or regional emissions. After their on-site deployment they are again measured at SIO to obtain an “in” value, to assess any possible drifts. They are also measured on-site against the previous and next tertiaries. The secondary standards and the synthetic primary standards at SIO provide the core of the AGAGE calibration system (Prinn et al., 2000; Miller et al., 2008).

The GC-MS-Medusa measurement precisions for HFC-23 and HCFC-22 are determined as the precisions of replicate measurements of the quaternary standards over twice the time interval as for sample-standard comparisons (Miller et al., 2008). Accordingly, they are upper-limit estimates of the precisions of the sample-standard comparisons. Typical daily precisions for each compound vary with abundance and individual instrument performance over time. Average percentage relative standard deviation (% RSD) between 2007 and 2016 were: HFC-23 (0.1%-1.9%, average 0.7%); and for HCFC-22 (0.1%-2.5%, average 0.6%).

Supplementary Material (2): Firn Air Depth Profiles, Analyses of the CGAA and old Northern Hemisphere (NH) air samples

In this section we illustrate in Figures S1 the depth profiles for HFC-23 in the polar firn and in Figure S2 we show three independent analyses of the data from the CGAA. Tables S1 and S2 also list the actual data used to construct these figures.

Figure S1. Depth profiles for HFC-23 in polar firn. DSSW20K and SPO-01 are Antarctic sites and NEEM-08 is from Greenland. The modelled mole fractions correspond to the optimized emissions history using an inversion and firn air model developed at CSIRO.

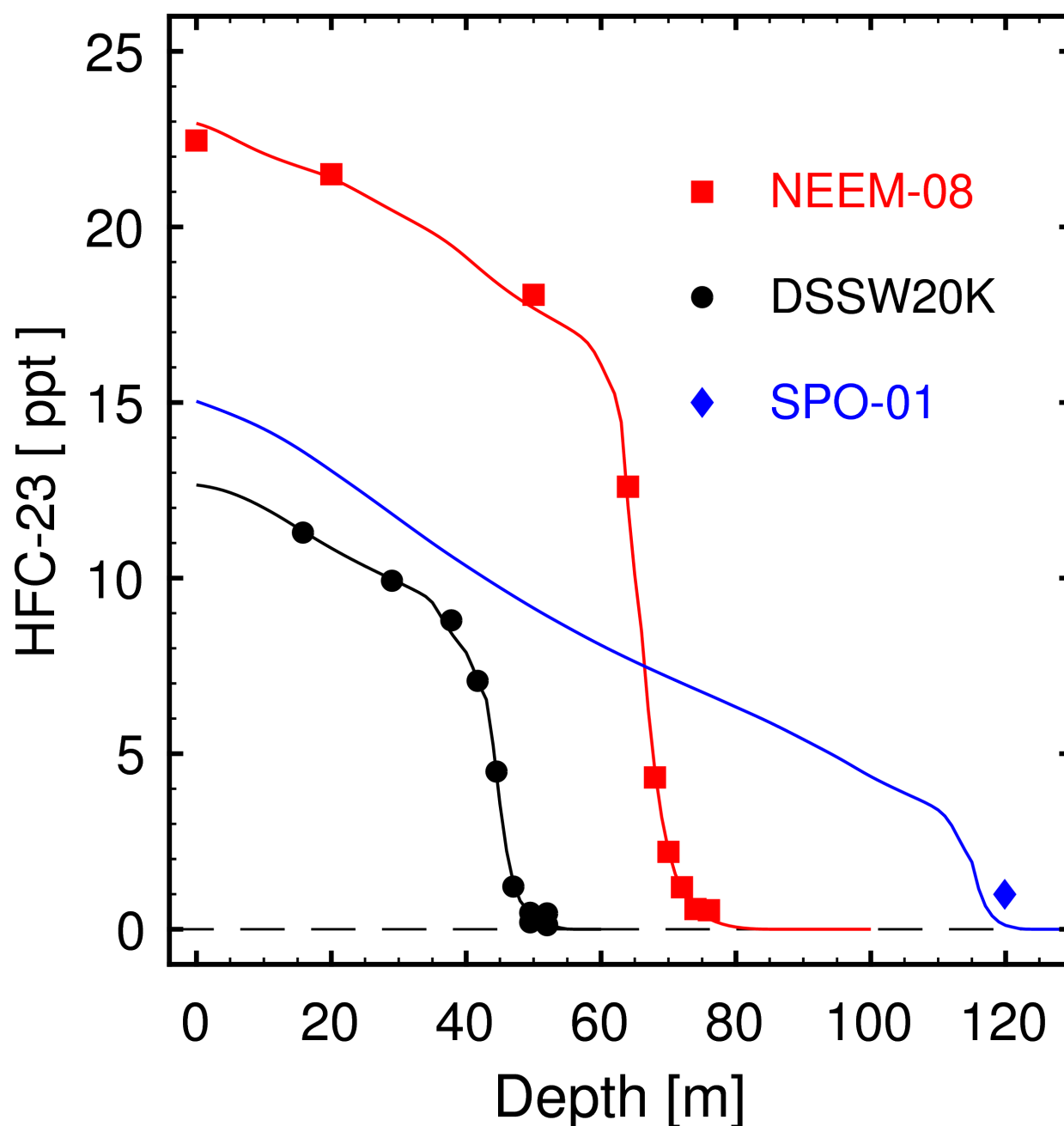
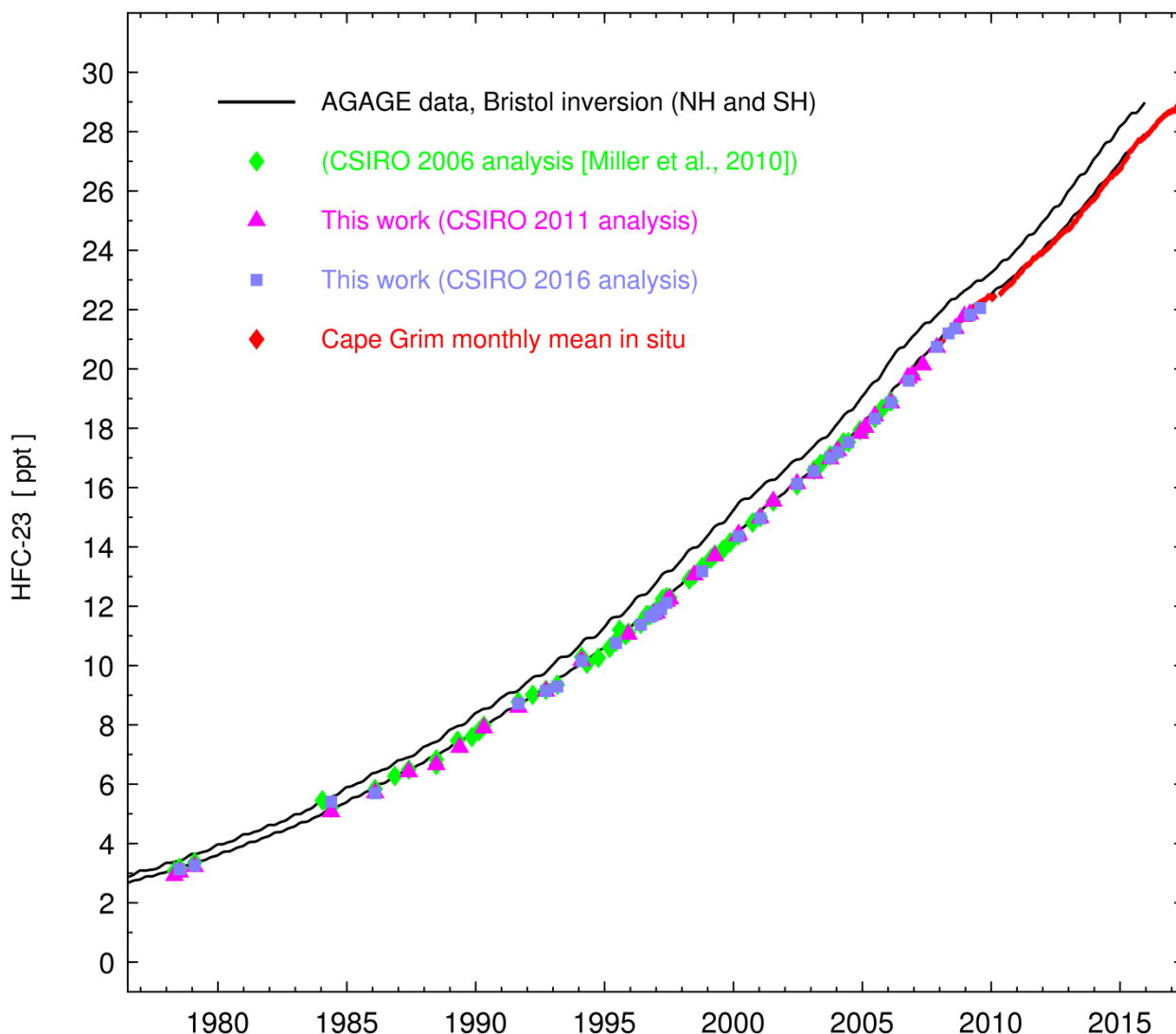


Figure S2. Comparison of three analysis sets of HFC-23 in the Cape Grim Air Archive



A series of old Northern Hemisphere (NH) air samples were mostly collected during clean air conditions but not with the purpose of creating a consistent air archive. Therefore, a stepwise tightening filtering algorithm was applied to the measurement results based on their deviations from a fit through all data (including in situ data). Due to the scarcity of the Northern Hemisphere HFC-23 data, the filtering of these samples used the fit through the filtered Southern Hemisphere samples as additional guide (with an appropriate time lag related to hemispheric transport). The remaining final NH HFC-23 data showed good agreement with concurrent in situ measurements. (Möhle et al., 2010; Vollmer et al., 2016)

Table S1

 Firm air measurement and model results for HFC-23

Abbreviations: m: measured; mf: mole fraction; p: precision (measurement repeatability, 1 sigma); mod: firm air model output with uncertainties

Primary calibration scale for HFC-23: SIO-07

depth: depth in firm air hole from which sample was drawn

Sample Volume: volume of sample used in one analysis on the Medusa-GCMS

Flags used for the decisions on presence of the compound in the sample

Flag 1: Peak size large enough a non-zero positive mole fraction was calculated and reported.

Flag 2: Clear sign of a peak but very small. Mole fraction was calculated by GCWerks either using generally set parameters or using GCWerks special integration

Flag 3: Maybe a peak some baseline disturbance that point to a non-zero signal. In most cases a mole fraction assigned

Flag 4: no sign of a peak at all no change in baseline. Mole fraction definitely smaller than the estimated detection limit for that sample

Site	Tank_ID	UAN	Parent_UAN	sample					HFC-23					
				depth	volume	m-mf	m-p	n	Flag	mod-mf	mod-min	mod-max	mean	effect
				[m]	[L]	[ppt]	[ppt]			[ppt]	[ppt]	[ppt]	Age	Age
DSSW20K	S22L-002	UAN980141	UAN980141	15.8	3	11.295	0.071	3	1	11.335	11.282	11.449	1995.95	1996.26
DSSW20K	MC-05	UAN980780	UAN980142	29	2	9.924	0.098	2	1	9.968	9.856	10.1	1993.63	1994.04
DSSW20K	CA01674	UAN980143	UAN980143	37.8	3	8.796	0.041	4	1	8.431	8.327	8.624	1990.64	1991.23
DSSW20K	MC-08	UAN980783	UAN980144	41.7	2	7.074	0.06	2	1	7.075	6.954	7.307	1987.71	1988.85

DSSW20K	MC-09	UAN980784	UAN980145	44.5	2	4.49	0.018	2	1	4.425	4.221	4.54	1980.51	1982.51
DSSW20K	MC-06	UAN980781	UAN980146	47	2	1.215	0.021	2	1	1.323	1.195	1.411	1966.83	1970.73
DSSW20K	MC-04	UAN980779	UAN980147	49.5	2	0.196	0.033	2	1	0.478	0.414	0.53	1952.95	1953.44
DSSW20K	S22L-010	UAN980148	UAN980148	49.5	1.5	0.468	0.061	2	1	0.478	0.414	0.53	1952.95	1953.44
DSSW20K	MC-01	UAN980776	UAN980150	52	2	0.128	0.011	2	1	0.478	0.414	0.53	1952.95	1953.44
DSSW20K	MC-10	UAN980785	UAN980149	52	1	0.451	0.064	2	1	0.478	0.414	0.53	1952.95	1953.44
DSSW20K	S22L-007	UAN980151	UAN980151	52	2	0.115	0	1	1	0.137	0.137	0.292	1938.93	1937.62
NEEM-2008	S300-B15	UAN999698	UAN999698	0	1.5	22.462	0.104	2	1	0.137	0.137	0.292	1938.93	1937.62
NEEM-2008	S300-B13	UAN999697	UAN999697	20	1.5	21.502	0.189	2	1	0.137	0.137	0.292	1938.93	1937.62
NEEM-2008	S300-B11	UAN999695	UAN999695	50	1.5	18.067	0.067	2	1	0.137	0.137	0.292	1938.93	1937.62
NEEM-2008	S300-B12	UAN999696	UAN999696	64	1.5	12.602	0.1	2	1	0.137	0.137	0.292	1938.93	1937.62
NEEM-2008	S300-B16	UAN999699	UAN999699	68	1.5	4.322	0.012	2	1	0.137	0.137	0.292	1938.93	1937.62
NEEM-2008	S300-B18	UAN999701	UAN999701	70	1.5	2.204	0.051	2	1	0.137	0.137	0.292	1938.93	1937.62
NEEM-2008	S300-B19	UAN999702	UAN999702	72	1.5	1.196	0.047	2	1	0.137	0.137	0.292	1938.93	1937.62
NEEM-2008	S300-B17	UAN999700	UAN999700	74	1.5	0.575	0.05	2	1	0.137	0.137	0.292	1938.93	1937.62
NEEM-2008	S300-B20	UAN999703	UAN999703	76	1.5	0.541	0.011	2	1	NaN	NaN	NaN	NaN	NaN
SPO	S300-A23	UAN996580	UAN993582	119.87	1	0.994	0.04	2	1	21.391	21.182	21.537	2006.96	2007

Table S1

Firn air measurement and model results for HFC-23

Abbreviations: m: measured; mf: mole fraction; p: precision (measurement repeatability, 1 sigma); mod: firn air model output with uncertainties

Primary calibration scale for HFC-23: SIO-07

depth: depth in firn air hole from which sample was drawn

Sample Volume: volume of sample used in one analysis on the Medusa-GCMS

Flags used for the decisions on presence of the compound in the sample

Flag 1: Peak size large enough a non-zero positive mole fraction was calculated and reported.

Flag 2: Clear sign of a peak but very small. Mole fraction was calculated by GCWerks either using generally set parameters or using GCWerks special integration

Flag 3: Maybe a peak some baseline disturbance that point to a non-zero signal. In most cases a mole fraction assigned

Flag 4: no sign of a peak at all no change in baseline. Mole fraction definitely smaller than the estimated detection limit for that sample

Site	Tank_ID	UAN	Parent_UAN	sample					HFC-23					
				depth	volume	m-mf	m-p	n	Flag	mod-mf	mod-min	mod-max	mean	effect
				[m]	[L]	[ppt]	[ppt]			[ppt]	[ppt]	[ppt]	Age	Age
DSSW20K	S22L-002	UAN980141	UAN980141	15.8	3	11.295	0.071	3	1	11.335	11.282	11.449	1995.95	1996.26
DSSW20K	MC-05	UAN980780	UAN980142	29	2	9.924	0.098	2	1	9.968	9.856	10.1	1993.63	1994.04
DSSW20K	CA01674	UAN980143	UAN980143	37.8	3	8.796	0.041	4	1	8.431	8.327	8.624	1990.64	1991.23
DSSW20K	MC-08	UAN980783	UAN980144	41.7	2	7.074	0.06	2	1	7.075	6.954	7.307	1987.71	1988.85

DSSW20K	MC-09	UAN980784	UAN980145	44.5	2	4.49	0.018	2	1	4.425	4.221	4.54	1980.51	1982.51
DSSW20K	MC-06	UAN980781	UAN980146	47	2	1.215	0.021	2	1	1.323	1.195	1.411	1966.83	1970.73
DSSW20K	MC-04	UAN980779	UAN980147	49.5	2	0.196	0.033	2	1	0.478	0.414	0.53	1952.95	1953.44
DSSW20K	S22L-010	UAN980148	UAN980148	49.5	1.5	0.468	0.061	2	1	0.478	0.414	0.53	1952.95	1953.44
DSSW20K	MC-01	UAN980776	UAN980150	52	2	0.128	0.011	2	1	0.478	0.414	0.53	1952.95	1953.44
DSSW20K	MC-10	UAN980785	UAN980149	52	1	0.451	0.064	2	1	0.478	0.414	0.53	1952.95	1953.44
DSSW20K	S22L-007	UAN980151	UAN980151	52	2	0.115	0	1	1	0.137	0.137	0.292	1938.93	1937.62
NEEM-2008	S300-B15	UAN999698	UAN999698	0	1.5	22.462	0.104	2	1	0.137	0.137	0.292	1938.93	1937.62
NEEM-2008	S300-B13	UAN999697	UAN999697	20	1.5	21.502	0.189	2	1	0.137	0.137	0.292	1938.93	1937.62
NEEM-2008	S300-B11	UAN999695	UAN999695	50	1.5	18.067	0.067	2	1	0.137	0.137	0.292	1938.93	1937.62
NEEM-2008	S300-B12	UAN999696	UAN999696	64	1.5	12.602	0.1	2	1	0.137	0.137	0.292	1938.93	1937.62
NEEM-2008	S300-B16	UAN999699	UAN999699	68	1.5	4.322	0.012	2	1	0.137	0.137	0.292	1938.93	1937.62
NEEM-2008	S300-B18	UAN999701	UAN999701	70	1.5	2.204	0.051	2	1	0.137	0.137	0.292	1938.93	1937.62
NEEM-2008	S300-B19	UAN999702	UAN999702	72	1.5	1.196	0.047	2	1	0.137	0.137	0.292	1938.93	1937.62
NEEM-2008	S300-B17	UAN999700	UAN999700	74	1.5	0.575	0.05	2	1	0.137	0.137	0.292	1938.93	1937.62
NEEM-2008	S300-B20	UAN999703	UAN999703	76	1.5	0.541	0.011	2	1	NaN	NaN	NaN	NaN	NaN
SPO	S300-A23	UAN996580	UAN993582	119.87	1	0.994	0.04	2	1	21.391	21.182	21.537	2006.96	2007

Table S2

Cape Grim Air Archive (CGAA) Results for HFC-23 from three analysis periods

Results are reported as dry air mole fractions for abundance (c) and precisions (p)

Measurements are conducted on the CSIRO Aspendale-9 GCMS-Medusa

Primary calibration scales: CFC-23: SIO-07

Notes for 2006: Measurements by B. R. Miller, L. Porter, L. P. Steele, P. B. Krummel. Results by peak area. Standard is G-141 with assigned values: CFC-23: 19.648 ppt

Notes for 2011: Measurements by D. Ivy, L. P. Steele, P. B. Krummel, M. Leist, Results by peak area. Standard is G-181 with assigned values: CFC-23: 23.1456 ppt

Notes for 2016: Measurements by M. K. Vollmer, L. P. Steele, B. Mitrevski, P. B. Krummel, Results by peak area. Standard is E-146S with assigned values: CFC-23: 31.4808 ppt

sampleID	time	year	month	day	c_mean	p_mean	c_2006	p_2006	n_2006	c_2011	p_2011	n_2011	c_2016	p_2016	n_2016
	fractional				[ppt]	[ppt]	[ppt]	[ppt]		[ppt]	[ppt]		[ppt]	[ppt]	
UAN780001	1978.315	1978	4	26	2.992	0.081	3.065	0.114	3	2.918	0.048	3	NaN	NaN	NaN
UAN780002	1978.512	1978	7	7	3.116	0.018	3.178	0.023	3	3.037	0.009	3	3.133	0.023	3
UAN790001	1979.099	1979	2	6	3.282	0.025	3.363	0.027	3	3.223	0.04	3	3.259	0.008	3
UAN910377	1984.053	1984	1	20	5.453	0.044	5.453	0.044	2	NaN	NaN	NaN	NaN	NaN	NaN
UAN840004	1984.391	1984	5	23	5.226	0.023	5.2	0.034	4	5.066	0.021	4	5.411	0.014	3
UAN860001	1986.099	1986	2	6	5.746	0.048	5.835	0.046	4	5.71	0.086	4	5.694	0.012	3
UAN860005	1986.863	1986	11	12	6.275	0.142	6.275	0.142	4	NaN	NaN	NaN	NaN	NaN	3

UAN870006	1987.403	1987	5	28	6.456	0.06	6.493	0.039	4	6.418	0.08	6	NaN	NaN	NaN
UAN880003	1988.47	1988	6	21	6.651	0.058	6.646	0.065	6	6.657	0.051	3	NaN	NaN	NaN
UAN880002	1988.47	1988	6	21	6.834	0.037	6.834	0.037	4	NaN	NaN	NaN	NaN	NaN	3
UAN890002	1989.299	1989	4	20	7.466	0.04	7.466	0.04	4	NaN	NaN	NaN	NaN	NaN	NaN
UAN890004	1989.378	1989	5	19	7.24	0.083	NaN	NaN	NaN	7.24	0.083	8	NaN	NaN	3
UAN890005	1989.852	1989	11	8	7.589	0.064	7.589	0.064	4	NaN	NaN	NaN	NaN	NaN	NaN
UAN900027	1990.127	1990	2	16	7.786	0.145	7.786	0.145	4	NaN	NaN	NaN	NaN	NaN	NaN
UAN900048	1990.315	1990	4	26	7.932	0.112	7.969	0.06	5	7.894	0.164	3	NaN	NaN	3
UAN910361	1991.658	1991	8	29	8.695	0.06	8.775	0.057	3	8.592	0.09	3	8.718	0.032	3
UAN920469	1992.211	1992	3	18	9.012	0.025	9.012	0.025	3	NaN	NaN	NaN	NaN	NaN	NaN
UAN920655	1992.727	1992	9	23	9.152	0.049	9.18	0.042	4	9.135	0.059	5	9.14	0.046	3
UAN930279	1993.164	1993	3	2	9.321	0.023	9.353	0.024	3	NaN	NaN	NaN	9.289	0.023	3
UAN940378	1994.112	1994	2	11	10.205	0.054	10.291	0.077	3	10.17	0.072	3	10.154	0.012	3
UAN940679	1994.318	1994	4	27	10.06	0.043	10.06	0.043	3	NaN	NaN	NaN	NaN	NaN	NaN
UAN941096	1994.759	1994	10	4	10.259	0.192	10.259	0.192	4	NaN	NaN	NaN	NaN	NaN	NaN
UAN950527	1995.195	1995	3	13	10.596	0.023	10.596	0.023	4	NaN	NaN	NaN	NaN	NaN	NaN
UAN950789	1995.447	1995	6	13	10.788	0.059	10.82	0.088	6	NaN	NaN	NaN	10.756	0.03	3
UAN950894	1995.584	1995	8	2	11.202	0.157	11.202	0.157	4	NaN	NaN	NaN	NaN	NaN	NaN
UAN960115	1995.811	1995	10	24	11.027	0.109	11.027	0.109	4	NaN	NaN	NaN	NaN	NaN	NaN
UAN960051	1995.923	1995	12	4	11.081	0.052	11.108	0.06	3	11.054	0.044	5	NaN	NaN	NaN
UAN960957	1996.404	1996	5	28	11.39	0.056	11.407	0.068	5	NaN	NaN	NaN	11.373	0.043	3

UAN961164	1996.637	1996	8	21	11.705	0.123	11.705	0.123	3	NaN	NaN	NaN	NaN	NaN	NaN
UAN961409	1996.754	1996	10	3	11.668	0.04	11.695	0.074	3	NaN	NaN	NaN	11.64	0.006	3
UAN970092	1996.885	1996	11	20	11.728	0.044	11.766	0.069	4	11.726	0.031	4	11.693	0.033	3
UAN970008	1997.016	1997	1	7	11.809	0.06	11.871	0.114	5	11.767	0.051	5	11.79	0.016	3
UAN970011	1997.016	1997	1	7	11.813	0.081	11.824	0.123	3	NaN	NaN	NaN	11.802	0.039	3
UAN970010	1997.017	1997	1	7	11.812	0.062	11.812	0.062	3	NaN	NaN	NaN	NaN	NaN	NaN
UAN970380	1997.195	1997	3	13	11.934	0.063	11.97	0.085	13	NaN	NaN	NaN	11.898	0.041	6
UAN970754	1997.255	1997	4	4	12.245	0.071	12.245	0.071	4	NaN	NaN	NaN	NaN	NaN	NaN
UAN970756	1997.408	1997	5	30	12.194	0.046	12.3	0.093	5	12.17	0.019	4	12.112	0.027	3
UAN971115	1997.534	1997	7	15	12.263	0.057	12.281	0.044	3	12.244	0.07	7	NaN	NaN	NaN
UAN980724	1998.285	1998	4	15	12.902	0.116	12.902	0.116	5	NaN	NaN	NaN	NaN	NaN	NaN
UAN980918	1998.479	1998	6	25	13.052	0.081	13.051	0.086	6	13.053	0.077	5	NaN	NaN	NaN
UAN981563	1998.786	1998	10	15	13.25	0.062	13.323	0.091	15	NaN	NaN	NaN	13.177	0.032	3
UAN991060	1999.129	1999	2	17	13.606	0.089	13.606	0.089	6	NaN	NaN	NaN	NaN	NaN	NaN
UAN991062	1999.279	1999	4	13	13.717	0.067	13.737	0.026	4	13.696	0.108	5	NaN	NaN	NaN
UAN991381	1999.59	1999	8	4	13.904	0.088	13.904	0.088	3	NaN	NaN	NaN	NaN	NaN	NaN
UAN992045	1999.874	1999	11	16	14.152	0.11	14.152	0.11	5	NaN	NaN	NaN	NaN	NaN	NaN
UAN20101335	2000.164	2000	3	1	14.375	0.088	NaN	NaN	NaN	14.375	0.088	6	NaN	NaN	NaN
UAN992982	2000.199	2000	3	14	14.391	0.092	14.393	0.139	6	14.426	0.111	5	14.353	0.028	3
UAN993562	2000.744	2000	9	29	14.818	0.044	14.818	0.044	4	NaN	NaN	NaN	NaN	NaN	NaN
UAN993563	2001.038	2001	1	15	14.979	0.089	15.002	0.111	7	14.977	0.133	4	14.957	0.022	3

UAN994885	2001.545	2001	7	19	15.534	0.104	15.53	0.116	3	15.539	0.093	5	NaN	NaN	NaN
UAN994886	2002.466	2002	6	20	16.11	0.075	16.08	0.105	4	16.13	0.086	6	16.121	0.035	3
UAN995445	2003.129	2003	2	17	16.54	0.071	16.596	0.08	6	16.481	0.079	5	16.544	0.053	3
UAN996454	2003.384	2003	5	21	16.802	0.071	16.802	0.071	3	NaN	NaN	NaN	NaN	NaN	NaN
UAN996455	2003.753	2003	10	3	17.018	0.062	17.081	0.096	4	16.967	0.057	5	17.005	0.032	3
UAN996456	2004.053	2004	1	20	17.265	0.113	17.265	0.113	3	NaN	NaN	NaN	NaN	NaN	NaN
UAN998318	2004.057	2004	1	22	17.237	0.058	17.275	0.072	5	17.24	0.059	6	17.195	0.042	3
UAN996457	2004.268	2004	4	8	17.523	0.205	17.523	0.205	3	NaN	NaN	NaN	NaN	NaN	NaN
UAN996458	2004.459	2004	6	17	17.529	0.025	17.53	0.026	3	NaN	NaN	NaN	17.529	0.025	3
UAN997089	2004.915	2004	12	1	17.879	0.075	17.932	0.075	16	17.826	0.075	18	NaN	NaN	NaN
UAN997090	2005.11	2005	2	10	18.009	0.037	17.991	0.052	5	18.028	0.021	5	NaN	NaN	NaN
UAN998005	2005.488	2005	6	28	18.36	0.098	18.345	0.175	14	18.413	0.095	18	18.32	0.025	6
UAN998006	2005.759	2005	10	5	18.653	0.122	18.653	0.122	8	NaN	NaN	NaN	NaN	NaN	NaN
UAN998195	2006.11	2006	2	10	18.873	0.134	18.905	0.204	14	18.853	0.173	15	18.862	0.025	6
G-139	2006.756	2006	10	4	19.695	0.12	NaN	NaN	NaN	19.695	0.12	6	NaN	NaN	NaN
UAN998425	2006.797	2006	10	19	19.65	0.042	NaN	NaN	NaN	19.696	0.043	6	19.603	0.042	4
UAN998852	2006.942	2006	12	11	19.784	0.094	19.778	0.134	5	19.791	0.054	4	NaN	NaN	NaN
UAN998898	2007.348	2007	5	8	20.132	0.098	NaN	NaN	NaN	20.132	0.098	5	NaN	NaN	NaN
UAN999276	2007.89	2007	11	22	20.733	0.181	NaN	NaN	NaN	20.726	0.308	5	20.741	0.054	3
UAN999627	2008.347	2008	5	7	21.198	0.014	NaN	NaN	NaN	NaN	NaN	NaN	21.198	0.014	3
UAN999756	2008.612	2008	8	12	21.365	0.067	NaN	NaN	NaN	21.364	0.086	6	21.365	0.049	3

UAN20100047	2008.956	2008	12	16	21.773	0.071	NaN	NaN	NaN	21.773	0.071	5	NaN	NaN	NaN
UAN20100609	2009.175	2009	3	6	21.836	0.09	NaN	NaN	NaN	21.851	0.118	8	21.821	0.062	3
UAN20101456	2009.567	2009	7	27	22.051	0.031	NaN	NaN	NaN	NaN	NaN	NaN	22.051	0.031	3

Supplementary Material (3): Emissions Inventories

HFC-23 (trifluoromethane, fluoroform, CHF_3) is a by-product of the chemical process to manufacture HCFC-22 (chlorodifluoromethane, CHClF_2) from chloroform and hydrogen fluoride.

S3.1. HCFC-22 Production

HCFC-22 is used in two ways: the commercial product is used in the refrigeration and air conditioning industries, and is eventually emitted into the atmosphere; production and consumption for this are controlled under the Montreal Protocol. It is also a chemical feedstock, the raw material for the manufacture of PTFE (polytetrafluoroethylene) and other fluoropolymers, effectively being destroyed in the process with small, inadvertent emissions not controlled under the Montreal Protocol.

Table S3 shows the inventory of HCFC-22 production for all end uses, subdivided between developed countries (referred to in the Montreal Protocol as "non-Article 5 countries", that are not eligible for any support under the Montreal Protocol or United Nations Framework Convention on Climate Change (UNFCCC) mechanisms, and individual Article 5 countries that are eligible to receive support to reduce emissions of HFC-23.

In the case of the non-A5 countries (which are listed individually in Table S4), historical demand for dispersive uses was taken from the AFEAS database ⁽¹⁾ up to 2007 and demand for fluoropolymer feedstock was derived from Stanford Research Institute data ⁽²⁾ that shows historical linear growth at 5800 tonnes/year from 2001 onwards and a requirement of about 50% of the reported dispersive demand up to that date. Production for dispersive use in 2008 was derived from the Parties submissions to the Montreal Protocol ⁽³⁾ and the Technology and Economic Assessment Panel of the Montreal Protocol ⁽⁴⁾. From 2009 onwards, the total production reported to the Executive Committee of the Montreal Protocol was used ⁽⁵⁾.

The same report to the Executive Committee ⁽⁵⁾ was used for production from individual Article 5 countries from 2009 onwards; prior to that year, the quantities produced in Argentina, India, South Korea, Mexico and Venezuela were estimated using the Montreal Protocol and TEAP data ^(3, 4).

Table S3. Estimated HCFC-22 production: Total for all uses Gg.

Year	Non-Article 5 Countries	Article 5 Countries						Global Total	
		Argentina	China	India	Korea (N)	Korea (S)	Mexico		Venezuela
1990	320.57	0	0	3.62	0	1.75	1.54	1.85	329.33
1990	320.57	0	0	3.62	0	1.75	1.54	1.85	329.33
1991	355.22	0	0	3.86	0	2.65	1.84	1.80	365.37
1992	368.57	0	0	3.72	0	3.97	1.86	2.04	380.16
1993	360.93	0.18	4.92	4.72	0	4.41	2.82	2.01	379.99
1994	359.17	0.21	9.83	4.50	0	4.51	2.14	1.43	381.79
1995	365.20	0.00	14.75	5.22	0	5.09	1.96	1.45	393.67
1996	406.86	0.00	19.66	4.54	0	8.27	4.80	1.39	445.53
1997	376.66	0.00	24.58	5.33	0	9.28	4.67	1.37	421.89
1998	391.76	0.00	37.14	8.34	0	7.88	3.42	0.95	449.48
1999	378.56	0.00	59.74	8.68	0	14.42	4.89	1.07	467.37
2000	365.77	0.11	77.79	11.18	0	11.29	3.43	1.20	470.77
2001	345.20	0.11	111.42	12.01	0	5.81	2.59	1.32	478.46
2002	331.76	0.58	103.37	11.26	0	10.22	3.81	1.44	462.44
2003	326.63	1.06	144.22	13.88	0	6.84	3.70	1.57	497.89
2004	334.73	1.54	191.06	17.99	0	5.53	3.73	1.69	556.26
2005	327.37	2.01	270.89	17.41	0	7.92	5.53	1.81	632.93
2006	322.29	2.49	325.28	21.06	0	5.23	7.33	1.94	685.61
2007	328.10	2.96	414.97	29.32	0	4.94	9.13	2.06	791.47
2008	333.92	3.44	373.17	38.49	0	5.93	10.93	2.18	768.05
2009	195.80	3.91	483.98	47.66	0.50	6.91	12.73	2.31	753.80
2010	229.86	4.25	549.27	47.61	0.50	7.63	12.62	2.17	853.91
2011	241.78	4.02	596.98	48.48	0.48	7.26	11.81	2.44	913.26
2012	219.91	4.19	644.49	48.18	0.52	5.70	7.87	2.91	933.77
2013	193.52	1.95	615.90	40.65	0.58	6.67	7.38	2.20	868.86
2014	210.04	2.29	623.90	54.94	0.53	6.83	9.21	1.57	909.30
2015	225.16	2.45	534.93	53.31	0.50	7.18	4.75	0.68	828.95

Chinese production now accounts for 65% of the global total, with a large demand for fluoropolymer feedstock, and was estimated separately. Production for dispersive uses and export was derived from the submission to the Montreal Protocol database and TEAP data^(3, 4). Fluoropolymer (mainly polytetrafluoroethylene, PTFE) production from 1998 to 2002 was reported in China Chemical Reporter (CCR)⁽⁶⁾ and showed growth of 33%/year. This growth was assumed to be maintained until 2007, implying production of over 69 Gg/year of PTFE in 2007, a value consistent with the capacity for fluoropolymers stated in the 11th Chinese 5 year plan to be 80 Gg/year in 2007/8⁽⁷⁾. Total production of HCFC-22 in China was also reported in CCR⁽⁶⁾, with a growth rate of between 47% and 25% in the period 1998 to 2001. For the values calculated here, a subsequent growth rate of 15% / year was applied until 2008, and from 2009 onwards, the total annual productions reported to the Executive Committee of the Montreal Protocol were used⁽⁵⁾. The resulting values agree within 4% with the numbers for 2013 to 2015 reported separately by the Chinese government⁽⁸⁾.

S3.2. HFC-23 Emissions

Attempts to reduce HFC-23 formation by adjusting process conditions have important economic consequences for HCFC-22 production; the historic rate of HFC-23 production from a plant optimised for HCFC-22 production is 4%⁽⁹⁾. In plants, constructed in the last 10 years, this has been reduced to about 3%⁽⁵⁾. HFC-23 has few uses, some of which (for example, as a fire suppressing agent) will result in the eventual emission of most or all into the atmosphere. In the 21st century emissions from these uses have been almost constant at 133 ± 9 metric tonnes year⁻¹, a maximum of 10% of all emissions⁽¹⁰⁾. Prevention of emissions of HFC-23 requires the capture and treatment of the process vent stream, generally accomplished by high temperature oxidation.

Developed country signatories to the United Nations Framework Convention on Climate Change (UNFCCC), essentially the same set as the non-A5 countries, are required to report emissions of each HFC greenhouse gas each year. The emissions reported by individual countries are shown in the first columns of Table S4 ⁽¹⁰⁾; changes in accounting procedure, such as happened in Germany from 2007 were accommodated by using the original contemporaneous data files (rather than the compendia published in 2017). This is consistent with the step changes, that resulted either from closure of the HCFC-22 production facility or from capture and thermal oxidation of the HFC-23, and with pollutant reports to national authorities ^(11, 12).

The second set of columns in Table S4 shows the estimated emissions of HFC-23 from those countries that are eligible for assistance under the Clean Development Mechanism (CDM) of the UNFCCC. Essentially, this rewarded destruction of HFC-23 at 11700 times the value of the same mass of CO₂, a gearing ratio that distorted the economics of HCFC-22 production ⁽¹³⁾ and led to the closure of the CDM to HFC-23 projects after 2009. The decision of the EU to ban the use of HFC-23 certified emission reduction (CER) credits in the European Union Emissions Trading System from 1 May 2013 effectively rendered these CERs valueless ⁽⁵⁾.

The emissions in Table S4 were calculated by estimating the annual production of HFC-23 for each country and then subtracting the quantity estimated to have been abated.

Argentina and Mexico - from 1990 to 2011, production of HFC-23 was estimated at 3.6%, falling to 3% of HCFC-22 production; from 2012 to 2015, the actual productions reported by the Executive Committee of the Montreal Protocol ⁽⁵⁾ were used. This was abated up to the maximum claimed under the CDM ⁽¹⁴⁾ up to May 2013, after which the destruction facilities were apparently shut down and the HFC-23 was released into the atmosphere ⁽⁵⁾.

China - from 1990 to 2006, a production rate of 3.6% was assumed, falling to 2.8% subsequently ⁽⁵⁾. Abatement at the maximum rate allowed for the 11 of 32 plants operating under the CDM was then assumed until 2012 with the other 21 plants operating without abatement. From 2012 onwards, the actual emissions reported by China were used ⁽⁵⁾. The quantities of HFC-23 destroyed in the period 2007 to 2015 varied between 28 and 47% of that produced.

India - up to year 2000, a production rate of 3.6% was assumed, which then dropped to 2.9%. Apparently, all of the India plants have abatement technology and, after 2006, no emissions were estimated.

South Korea - a production rate of 4%, falling to 3% was assumed for the period 1990 to 2008. Subsequently the production reported to the Executive Committee was used ⁽⁵⁾. This was abated at the maximum allowed within the CDM until 2012, when the destruction facility was shut down. Although the HFC-23 is recovered for sale, much of that will be emitted and this is reflected in the values shown for South Korea.

North Korea - there are no data prior to 2009 and defaults of zero have been used. From 2009 onwards, the estimates here are those given in Reference 5, with total emission.

Venezuela - the production rate throughout is set at 3%, with no abatement.

Table S4. National HFC-23 Emissions (Metric tonnes Mt or Mg)

Year	Countries Reporting to UNFCCC under CRF											Countries Reporting Data under CDM							Total Annual Emission Gg	
	Australia	Canada	France	Germany	Greece	Italy	Japan	Netherlands	Russia	Spain	UK	USA	Argentina	China	India	Korea (N)	Korea (S)	Mexico		Venezuela
1990	48.1	65.6	142.0	373.4	79.9	30.0	717.6	378.8	2428.2	205.4	972.3	3127.6	0.0	0.0	130.4	0.0	70.0	55.5	55.4	8.88
1991	96.3	71.4	184.6	342.9	94.6	30.0	1140.3	295.0	2312.8	186.2	1012.3	2812.0	0.0	0.0	138.9	0.0	106.1	66.1	54.0	8.94
1992	93.2	56.1	173.7	342.4	77.6	30.0	1185.7	378.0	1904.6	236.1	1052.4	3123.9	0.0	0.0	134.0	0.0	158.6	67.1	61.2	9.07
1993	106.9	0.0	177.5	342.1	137.3	30.0	1173.0	424.2	1234.3	193.0	1092.4	2846.9	5.4	176.9	170.0	0.0	176.4	101.4	60.4	8.45
1994	96.5	0.0	79.4	342.6	183.2	30.0	1248.8	544.2	1044.1	295.5	1132.5	2716.1	6.3	353.9	162.1	0.0	180.4	77.0	42.8	8.54
1995	65.4	0.1	19.5	302.8	278.0	30.8	1432.0	503.0	1042.3	396.5	1192.6	2843.7	0.0	530.8	187.9	0.0	223.1	70.4	43.5	9.16
1996	30.7	0.1	32.9	263.6	320.2	1.2	1422.3	611.9	917.5	432.4	1220.7	2690.9	0.0	707.8	163.4	0.0	330.9	172.9	41.7	9.36
1997	0.0	0.9	31.6	254.7	338.9	1.6	1328.5	621.8	1212.3	495.9	1330.8	2601.3	0.0	884.7	192.0	0.0	278.3	168.0	41.1	9.78
1998	0.0	0.3	20.6	246.5	373.6	2.5	1245.3	711.3	1468.2	437.1	1030.2	3411.2	0.0	1337.0	300.2	0.0	166.1	122.9	28.5	10.90
1999	0.1	0.4	38.7	233.5	430.9	2.5	1233.2	318.5	1523.2	511.5	409.9	2636.6	0.0	2175.8	312.6	0.0	311.2	176.2	32.2	10.35
2000	0.1	0.5	31.9	109.1	321.7	3.0	1149.7	223.8	1783.7	557.2	219.1	2468.6	3.4	2827.1	402.6	0.0	276.7	123.4	35.9	10.54
2001	0.1	0.5	33.0	99.6	275.1	3.4	933.7	41.9	1680.8	270.0	196.8	1702.6	3.2	4036.4	353.0	0.0	47.6	93.1	39.6	9.81
2002	0.1	0.5	34.2	110.1	277.2	3.9	667.1	62.4	1268.3	120.4	165.4	1819.0	17.5	3780.5	330.9	0.0	145.0	137.3	43.3	8.98
2003	0.1	0.6	23.4	53.8	232.8	4.6	527.7	37.8	933.5	176.0	158.9	1066.3	31.8	5274.9	408.0	0.0	145.2	133.0	47.0	9.26
2004	0.2	0.6	30.3	53.2	224.1	5.3	261.6	31.9	1160.8	98.8	29.4	1488.3	46.1	6945.8	365.0	0.0	46.0	134.3	50.7	10.97
2005	0.2	0.6	35.4	53.8	191.4	6.0	85.5	17.6	1217.7	92.2	28.0	1368.9	60.3	9916.5	50.1	0.0	117.5	199.0	54.4	13.50
2006	0.2	0.6	42.3	35.9	7.7	6.7	90.3	25.0	1045.8	109.4	17.2	1201.1	74.6	11132.2	0.0	0.0	37.0	0.0	58.1	13.88
2007	0.3	0.6	26.8	10.6	11.6	7.5	63.8	21.8	943.0	98.8	8.3	1470.0	0.0	7872.6	0.0	0.0	28.1	33.5	61.8	10.66
2008	0.3	0.6	29.0	9.5	12.6	8.3	71.5	19.2	955.9	101.7	4.7	1180.3	0.0	5726.7	0.0	0.0	57.8	82.7	65.5	8.33
2009	0.3	0.5	15.2	8.2	12.9	8.4	36.7	13.8	571.9	90.9	3.8	473.3	0.0	7848.3	0.0	9.1	87.4	126.6	69.2	9.38
2010	0.3	0.6	11.6	7.8	15.0	9.0	9.6	34.9	572.8	122.9	1.1	559.1	0.0	9165.0	0.0	9.0	109.0	124.0	65.0	10.82
2011	0.4	0.7	7.5	8.3	13.3	9.3	6.1	15.0	317.1	78.2	1.0	607.9	0.0	9961.3	0.0	8.6	97.9	104.4	73.3	11.31
2012	0.4	0.7	8.0	7.8	14.9	9.2	4.3	11.3	637.1	69.9	0.9	386.2	0.0	10753.9	0.0	8.4	51.1	8.1	87.4	12.06
2013	0.4	0.7	9.1	7.4	15.1	9.4	4.3	17.5	798.7	60.6	1.0	290.1	29.3	10841.1	0.0	10.6	100.1	88.0	66.1	12.35
2014	0.5	0.6	9.2	7.2	12.2	9.6	5.2	3.9	912.2	55.7	1.2	364.2	68.6	12492.5	0.0	7.8	205.0	202.8	47.0	14.41
2015	0.5	0.6	9.3	6.7	11.9	9.8	6.7	9.1	665.6	46.4	1.4	313.0	73.4	7481.8	0.0	7.4	204.0	100.8	20.3	8.97

Notes.

- ¹ Production of HCFC-22 up to 2007 in non-Article 5 countries downloadable from <https://agage.mit.edu/data/agage-data>
- ² Stanford Research Institute, International, 1998: Fluorocarbons, Sections 543.7001 to 543.7005 of *Chemical Economics Handbook*, SRI International, Menlo Park, USA, updated using Will R. and H. Mori, Fluorocarbons, Chemical Economics Handbook 543.7000 of SRI Consulting, Access Intelligence (www.sriconsulting.com), 2008.
- ³ Production and Consumption of Ozone Depleting Substances under the Montreal Protocol, 1986-2015, *United Nations Environment Programme*, available at <http://ozone.unep.org/en/data-reporting/data-centre>
- ⁴ UNEP 2006 Assessment Report of the Technology and Economic Assessment Panel, *United Nations Environment Programme*, Nairobi, 2006.
- ⁵ Key aspects related to HFC-23 by-product control technologies (Decision 78/5), Report to the Executive Committee of the Multilateral Fund for the Implementation of the Montreal Protocol, UNEP/OzL.Pro/ExCom/79/48 of 7 June 2017 available at ozone.unep.org
- ⁶ Market Report: Fluorochemical develops rapidly in China, *China Chemical Reporter*, 13, Sep 6, 2002.
- ⁷ Development and Forecast Report on China Fluorine Industry between 2007 and 2008, www.acunion.net, 2009.
- ⁸ Wang Kaixiang, HCFCs/HFCs Production in China, Foreign Economic Cooperation Office, FECO/MEP, May 2015.
- ⁹ Intergovernmental Panel on Climate Change. Revised 1996 Guidelines for National Greenhouse Gas Inventories, Reference manual, vol 3, *IPCC/IGES*, Kanagawa, Japan, 1996.
- ¹⁰ Data reported under the *Common Reporting Format* and in *National Inventory Reports* available at http://unfccc.int/national_reports/annex_i_ghg_inventories/national_inventories_submissions/items/10116.php.
- ¹¹ US EPA Facility Level Greenhouse Gas Emissions Data available at <https://ghgdata.epa.gov/ghgp/main.do>
- ¹² European Pollutant Release and Transfer Register (E-PRTR) available at <http://prtr.ec.europa.eu>
- ¹³ Munnings C., B. Leard and A. Bento, The net emissions impact of HFC-23 offset projects from the Clean Development Mechanism, Resources for the Future, Discussion Paper 16-01, 2016.
- ¹⁴ UNFCCC, Clean Development Mechanism Project Activities available at <http://cdm.unfccc.int/Projects/Index.html>

Supplementary Material (4): Influence of OH on the inversions.

Small differences were found in the derived emissions of HCFC-22, whereas, owing to its very long lifetime, negligible differences were found for HFC-23.

For HCFC-22, the magnitude of the difference when Rigby et al., (2017) OH was used versus an annually repeating OH concentration was much smaller than the derived uncertainty.

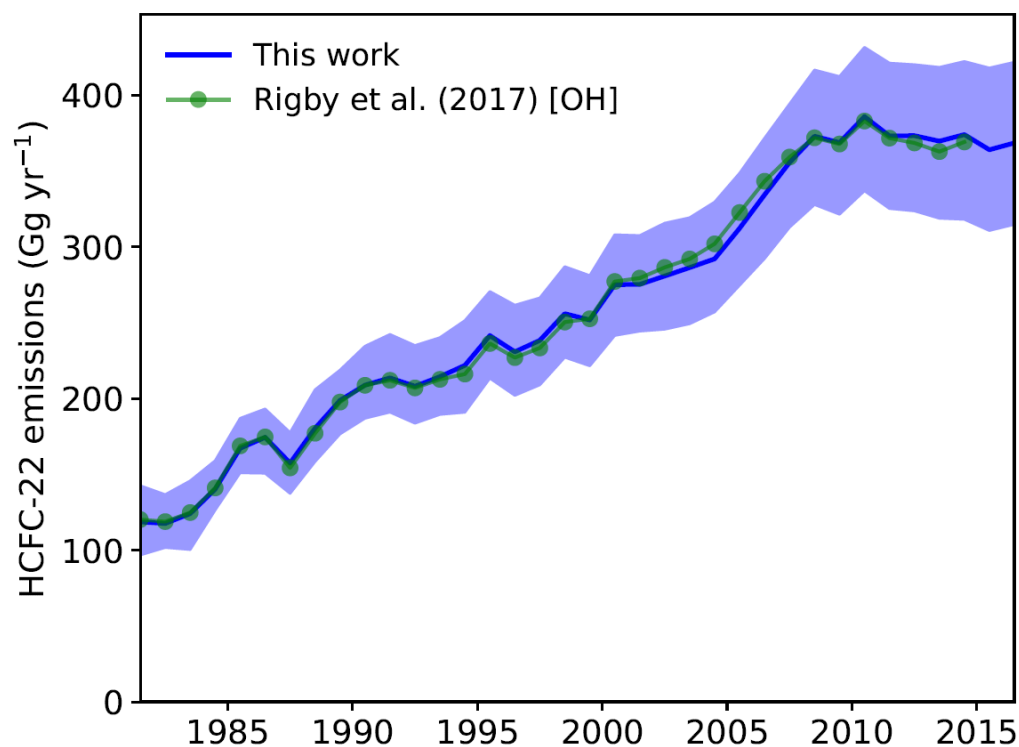


Figure S3. Potential variations in OH concentrations on the inversions

Supplementary Material (5): European Estimates Using FLEXPART and Empa Inversion

Detailed Results

The inversion results suggest that European emissions of HFC-23 in general were larger than reported to UNFCCC and exhibited considerable year-to-year variability. *A posteriori* estimates from the two inversions using different *a priori* emissions mostly agree with each other within the scope of their uncertainty limits (see Figure 6 in the main manuscript and Figure S4). Exceptions are the Italian estimates for the years 2013 and 2015, when the use of the UNFCCC *a-priori* resulted in much larger *a posteriori* emissions than the use of the ‘UNFCCC r0.5’ *a priori*. Furthermore, a large difference was also obtained for France in 2013, again the UNFCCC inversion yielding larger *a posteriori* emissions than the UNFCCC r0.5 inversion. All regions except Spain exhibited larger *a posteriori* than *a priori* emissions for all years. These differences were most significant for Italy where average *a posteriori* emissions of 38 ± 10 Mg/yr were estimated for the years 2009 to 2016. Although Italian *a posteriori* emissions were relatively low and closer to the *a priori* estimate in 2016 there is no clear negative trend in the emissions. Emissions from the Benelux region grew steadily until 2013 and dropped sharply afterwards, a tendency only partly reflected in the UNFCCC estimates. French *a posteriori* emissions agreed fairly well with the UNFCCC reports, with the exception of 2013 when at least one of the inversions yielded significantly higher emissions. A similar statement can be made for the United Kingdom, where only the *a posteriori* estimates for the year 2014 deviates more strongly from the UNFCCC values. The German *a posteriori* emissions were considerably larger than the *a priori* until 2012, thereafter they were closer to the reported UNFCCC values. Our *a posteriori* estimates for the Iberian Peninsula remained relatively close to the UNFCCC *a priori*. Total emissions for the six European regions listed in Table 4 (main manuscript) ranged from 108 ± 30 Mg/yr in 2015 up to 293 ± 43 Mg/yr in 2013 and showed a slightly negative, but insignificant trend for the period analysed here.

Compared to previous estimates by Keller et al. (2011) the estimates in this study for the years 2009 and 2010 are similar for Italy and the Benelux region, but were considerably smaller for Germany, France and the UK. The large difference for Germany may be explained by the much larger *a priori* estimate of 50 Mg/yr in Keller et al. (2011). For France and the UK similar *a priori* values were used and the differences may result from different selection of observation data. In Keller et al. (2011) the inversion was done for observations from July 2008 to July 2010, whereas here each inversion is based on one calendar year of observations.

The model performance was analysed at both Jungfraujoch and Mace Head with respect to correlations and root mean square error of simulated versus simulated time series (Figure S5). A large part of the correlation between simulation and observation is actually due to the increasing trend in HFC-23. Therefore, the correlation of the above-baseline signal can be seen as a better metric for the model performance. The latter increased considerably from *a-priori* to *a posteriori* for Jungfraujoch and only slightly for Mace Head. Again, there was

year-to-year variability in the correlation coefficient and for Jungfrauoch a tendency to smaller correlation coefficients for later years can be seen.

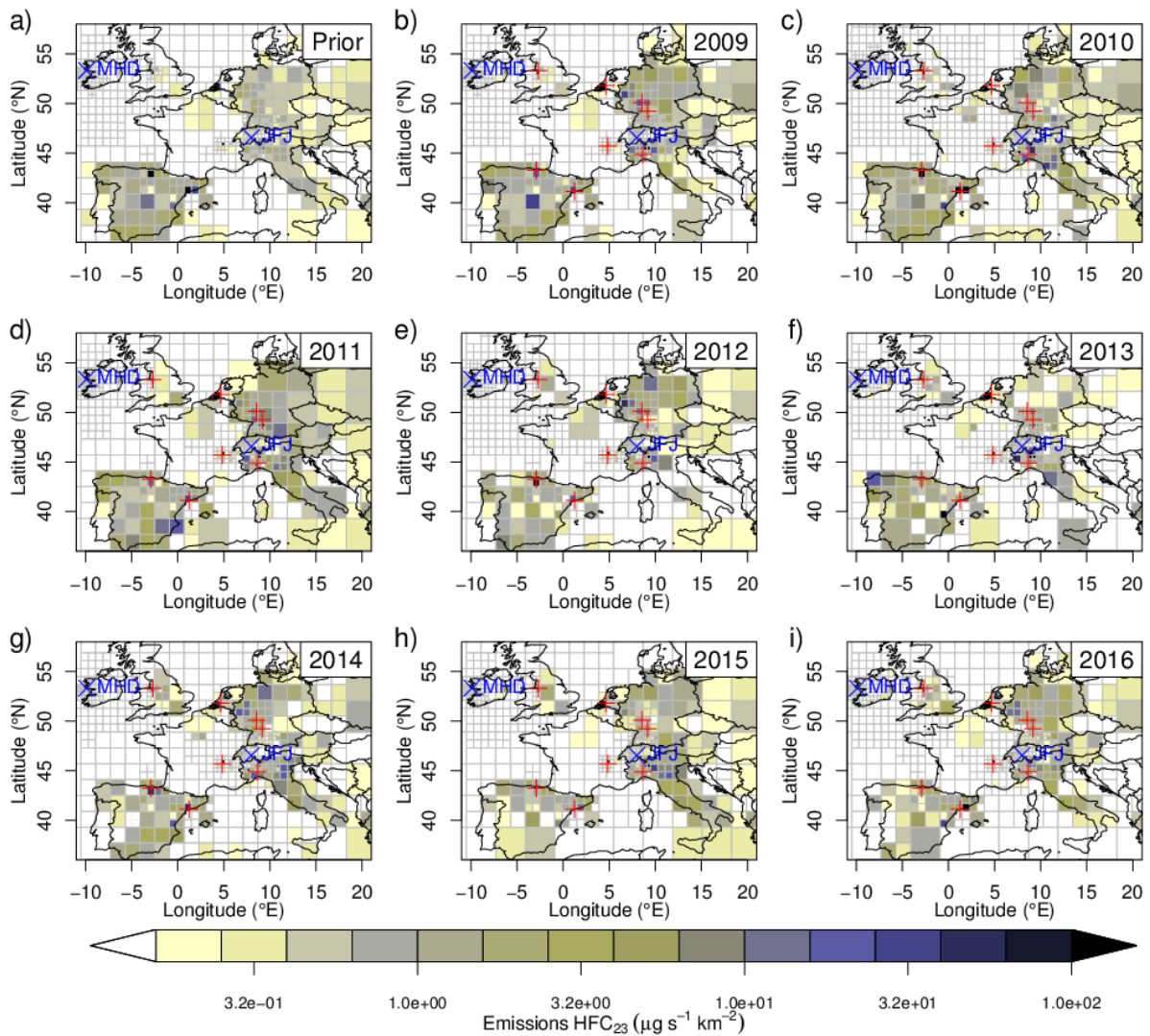


Figure S4: Spatial distribution of HFC-23 *a posteriori* emissions (b-i) as estimated when using the UNFCCC *a priori* emissions (a). Red crosses mark the location of past and present HCFC-22 production plants.

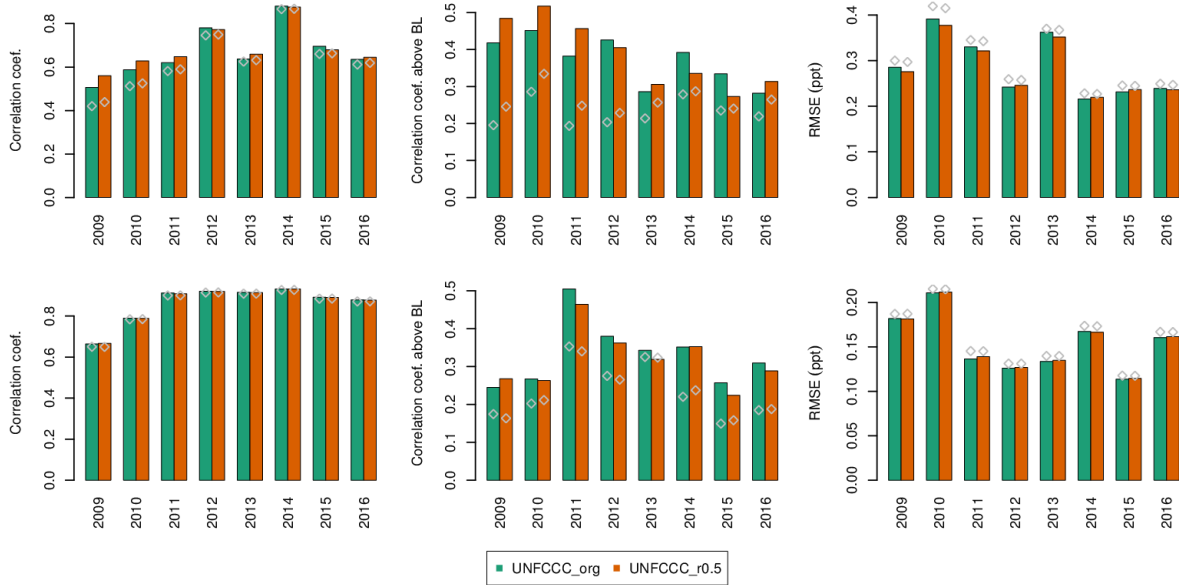


Figure S5: Regional scale transport model skills as evaluated against Jungfraujoch (top) and Mace Head (bottom) observations. *A priori* performance is shown as shaded bars and *a posteriori* performance as solid bars. (left) correlation coefficient for the complete time series, (centre) correlation coefficient for the regional (above baseline) part of the time series, (right) root mean square error.

References

Brunner, D., Arnold, T., Henne, S., Manning, A., Thompson, R. L., Maione, M., O'Doherty, S., and Reimann, S.: Comparison of four inverse modelling systems applied to the estimation of HFC-125, HFC-134a and SF₆ emissions over Europe, *Atmos. Chem. Phys. Discuss.*, 2017, 1-29, 2017.

Gridded Population of the World, Version 4 (GPWv4): Population Density Adjusted to Match 2015 Revision UN WPP Country Totals: <http://dx.doi.org/10.7927/H4HX19NJ>, 2016.
Henne, S., Brunner, D., Oney, B., Leuenberger, M., Eugster, W., Bamberger, I., Meinhardt, F., Steinbacher, M., and Emmenegger, L.: Validation of the Swiss methane emission inventory by atmospheric observations and inverse modelling, *Atmos. Chem. Phys.*, 16, 3683-3710, doi: 10.5194/acp-16-3683-2016, 2016.

Keller, C. A., Brunner, D., Henne, S., Vollmer, M. K., O'Doherty, S., and Reimann, S.: Evidence for under-reported western European emissions of the potent greenhouse gas HFC-23, *Geophys. Res. Lett.*, 38, L15808, doi: 10.1029/2011GL047976, 2011.

Seibert, P., and Frank, A.: Source-receptor matrix calculation with a Lagrangian particle dispersion model in backward mode, *Atmos. Chem. Phys.*, 4, 51-63, doi: 10.5194/acp-4-51-2004, 2004.

Stohl, A., Forster, C., Frank, A., Seibert, P., and Wotawa, G.: Technical note: The Lagrangian particle dispersion model FLEXPART version 6.2, *Atmos. Chem. Phys.*, 5, 2461-2474, doi: 10.5194/acp-5-2461-2005, 2005.

Supplementary Material (6): Additional HFC-23 emissions

Table S5. Annual mean global HFC-23 (CHF₃) emissions derived from the AGAGE 12-box model.

Year	HFC-23 Global annual emissions (Gg yr ⁻¹) ±1 sigma (σ) SD.	Year	HFC-23 Global annual emissions (Gg yr ⁻¹) ±1 sigma (σ) SD.
1930	0.54 ± 2.0	1955	0.11 ± 1.4
1931	0.52 ± 1.4	1956	0.16 ± 1.4
1932	0.50 ± 1.3	1957	0.20 ± 1.4
1933	0.47 ± 1.3	1958	0.29 ± 1.3
1934	0.44 ± 1.1	1959	0.39 ± 1.3
1935	0.41 ± 1.1	1960	0.43 ± 1.4
1936	0.37 ± 1.2	1961	0.50 ± 1.4
1937	0.34 ± 1.2	1962	0.62 ± 1.4
1938	0.30 ± 1.3	1963	0.76 ± 1.3
1939	0.27 ± 1.3	1964	0.92 ± 1.3
1940	0.24 ± 1.3	1965	1.10 ± 1.4
1941	0.20 ± 1.4	1966	1.33 ± 1.4
1942	0.17 ± 1.3	1967	1.60 ± 1.4
1943	0.15 ± 1.4	1968	1.94 ± 1.2
1944	0.12 ± 1.3	1969	2.15 ± 1.4
1945	0.09 ± 1.5	1970	2.24 ± 1.3
1946	0.07 ± 1.3	1971	2.38 ± 1.2
1947	0.05 ± 1.3	1972	2.61 ± 1.2
1948	0.04 ± 1.2	1973	2.95 ± 1.2
1949	0.03 ± 1.3	1974	2.98 ± 1.2
1950	0.02 ± 1.2	1975	2.99 ± 1.2
1951	0.01 ± 1.2	1976	2.95 ± 1.0
1952	0.02 ± 1.5	1977	3.17 ± 1.0
1953	0.04 ± 1.2	1978	3.62 ± 1.0
1954	0.06 ± 1.3	1979	3.92 ± 0.8

Arnold